

NAT'L INST. OF STAND & TECH. R.I.C.



A11104 551524

NBSIR 81-1638

NBS

PUBLICATIONS

EVALUATION OF A REVERBERATION CHAMBER FACILITY FOR PERFORMING EM RADIATED FIELDS SUSCEPTIBILITY MEASUREMENTS

Myron L. Crawford

Electromagnetic Fields Division
National Engineering Laboratory
National Bureau of Standards
Boulder, Colorado 80303

February 1981

QC
100
.U56
81-1638
1981
c.2

JUL 20 1981

not all - line

QC100

.U.S.G.

NO. 81-1638

1981

C.2

NBSIR 81-1638

EVALUATION OF A REVERBERATION CHAMBER FACILITY FOR PERFORMING EM RADIATED FIELDS SUSCEPTIBILITY MEASUREMENTS

Myron L. Crawford

Electromagnetic Fields Division
National Engineering Laboratory
National Bureau of Standards
Boulder, Colorado 80303

February 1981



U.S. DEPARTMENT OF COMMERCE, Malcolm Baldrige, Secretary

NATIONAL BUREAU OF STANDARDS, Ernest Ambler, Director

TABLE OF CONTENTS

	<u>Page</u>
List of Figures and Tables.....	iii
1.0 Introduction.....	1
2.0 Reverberating/Mode Tuned Chamber Theory of Operation.....	2
3.0 Description of TEMEC Measurement Setup and Procedure and NBS Evaluation System.....	5
4.0 TEMEC Analysis/Evaluation Results.....	7
4.1 Transmit and Receive Antennas VSWR.....	7
4.2 Chamber Coupling Efficiency/Insertion Loss.....	8
4.3 Test Zone E-Field Uniformity.....	8
4.4 E-Field Amplitude Calibration.....	9
5.0 Conclusions.....	10
6.0 Recommendations.....	11
7.0 Acknowledgments.....	12
8.0 References.....	13

LIST OF FIGURES AND TABLES

	<u>Page</u>
Figure 1. Cross sectional views of TEMEC (Mode Tuned Chamber)	14
Figure 2. Photograph of field tuner/stirrer installed in 2.4m x 3.0m x 7.6m shielded enclosure.....	15
Figure 3. Two dimensional graphic interpretation of modes inside resonant chamber.....	16
Figure 4. Mode tuned enclosure EMC measurement system.....	16
Figure 5. Block diagram of NBS modified mode tuned enclosure evaluation system for EMC measurements.....	17
Figure 6. NBS isotropic E-field probe and scanning system.....	18
Figure 7. Input VSWR of long wire transmit antenna as a function of tuner position.....	19
Figure 8. VSWR of transmitting and receiving antennas. Tuner in fixed position.....	22
Figure 9. VSWR of 10 dB attenuator-power detector used to measure received power from reference antenna.....	23
Figure 10. Minimum and average insertion loss of TEMEC (mode tuned chamber) with and without correction for net input power changes. Uncorrected based on incident power. Corrected based on net input power.....	24
Figure 11. Block diagram of system for evaluating E-field uniformity in test zone of TEMEC.....	25

Figure 12.	Cross sectional views of TEMEC showing location of transverse and longitudinal scans.....	26
Figure 13.	Results of E-field uniformity measurements taken along transverse scans through center of TEMEC test zone. Results are maximum amplitudes obtained from measurements made for complete revolution of tuner (unless otherwise indicated) as a function of probe position.....	27
Figure 14.	Results of E-field uniformity measurements taken along longitudinal scans through center of TEMEC test zone 0.914 m above floor. Results are maximum amplitude of E-field obtained from measurement of hermitian magnitude of E-field using NBS probe.....	30
Figure 15.	Results of E-field uniformity measurements made using NBS isotropic probe at 200 MHz. Computer based system used to correct for changes in net input power as a function of tuner and probe position. Scan made along length of chamber (longitudinal) through center of TEMEC test zone 0.914 m above floor.....	31
Figure 16.	E-field amplitude inside TEMEC as determined from NBS calibrated isotropic probe measurements. Probe located at center of chamber.....	32
Figure 17.	E-field amplitude inside TEMEC as determined from receiving antenna output power measurements.....	34
Figure 18.	Maximum and average E-field in TEMEC chamber as determined by NBS calibrated probe and receiving antenna power measurements. E_p determined from NBS probe measurements. E_A determined from receiving antenna power measurements.....	36
Figure 19.	Difference between E-field inside TEMEC as determined by NBS probe and receiving antenna power as a function of probe position along a longitudinal scan at center of test zone one meter above floor. Probe motion is from door end (receiving antenna location) toward transmit antenna (back).....	37
Table 1.	Potential resonant modes inside TEMEC (2.44m x 3.05m x 7.62m chamber) below 125 MHz.....	38
Table 2.	Summary of maximum variation in E-field along scans through TEMEC test zone. Scans ± 1 meter from center of chamber. E-field measured using NBS isotropic probe.....	38
Table 3.	Comparison of maximum E-field determined from NBS probe measurements made with a single dipole switched on and with all 3 orthogonal dipoles switched on (isotropic). Data gives maximum and minimum values of maximum E-field determined for a complete rotation of the mode tuner at discrete points along a transverse scan across the width of TEMEC (i.e., data shows influence of polarization of field in chamber).....	39
Table 4.	Difference between E-field determined from probe and receiving antenna measurements with and without correcting for net input power changes to transmitting antenna (i.e., error possible from failure to normalize probe and antenna output to net input power changes).....	39
Table 5.	Summary of difference between E-field amplitude determination inside TEMEC using NBS calibrated probe, E_p and receiving antenna, E_A . $\Delta E = E_p - E_A$	39

Evaluation of A Reverberation Chamber Facility for Performing EM Radiated Fields Susceptibility Measurements

Myron L. Crawford

Electromagnetic Fields Division
National Bureau of Standards
Boulder, Colorado 80303

This report describes measurement procedures and results for evaluation of a large 2.44m x 3.05m x 7.62m reverberating chamber facility in the frequency range (100-1000) MHz. This facility, referred to as a translational electromagnetic environment chamber, "TEMEC", is a mode tuned chamber developed for use in measuring electronic equipment susceptibility to EM radiated fields. A brief description of mode tuned cavity theory is given along with a description of the TEMEC measurement setup and the National Bureau of Standards modification of this setup for analysis and evaluation purposes. Measurements described include: (1) evaluation of the chamber's transmitting and receiving antenna voltage standing wave ratio; (2) measurement of the chamber's insertion loss or coupling efficiency versus frequency; (3) determination of E-field uniformity in the chamber test zone versus frequency; and (4) determination of the absolute amplitude calibration accuracy of the test fields in the chamber based upon the receiving antenna received power measurements.

Conclusions given indicate the chamber may be useful for performing electromagnetic susceptibility measurements at frequencies down to 200 MHz. E-field variations (time averaged) in the chambers test zone decrease from approximately 10 dB at 200-300 MHz to less than 3.7 dB at 1000 MHz and are anticipated to be less than 2 dB above 2 GHz. The uncertainty in establishing the absolute E-field amplitude in the chamber test zone is estimated to be less than 10 dB.

Key words: Electromagnetic radiated susceptibility measurements; mode tuned chamber; resonant cavity.

1.0 Introduction

Use of a mode tuned (reverberating) chamber for establishing electromagnetic (EM) fields is a relatively new method which appears to offer some unique advantages and potential for performing EM radiated susceptibility testing of electronic equipment. However, significant unanswered questions exist concerning the credibility of results obtained using this new method relative to correlation of the results to a free-space environment.

These questions basically fall into two categories. The first category relates to how well the chamber operates as a reverberating or highly moded chamber to establish time averaged (statistically) uniform, susceptibility test fields whose amplitude can be accurately determined as a function of test zone location and frequency. Measurements to evaluate this category of questions are performed with the chamber essentially empty (that is, no electronic equipment or test objects are placed inside which significantly interact or modify the EM field established inside the chamber). These measurements consist of:

(a) evaluating the chamber's transmitting and receiving (reference) antennas voltage standing wave ratios (VSWRs); (b) measuring the chamber loss or coupling efficiency versus frequency; (c) determining the E-field uniformity averaged over tuner position in the chamber test zone versus frequency; and (d) determining the absolute amplitude calibration accuracy of test fields in the chamber. Results of these measurements performed in the TEMEC chamber are contained in section 4 of this report, following a brief discussion of reverberation/mode tuned chamber theory of operation (section 2), and the description of the TEMEC measurement system, (section 3). Conclusions arrived at from the results given in section 4 are contained in section 5.

The second category of questions for evaluation relate to the interaction effects that exist between an equipment under test (EUT) placed inside the chamber and the ability, after inserting the EUT into the test chamber, to accurately characterize the test fields. Obviously, inserting an EUT into the chamber will influence the chamber quality factor or Q and its boundary condition, and hence will alter the field that was present before introducing the EUT. An additional question concerns the ability of the enclosure's complex field to couple to the EUT as compared to how a planar (far-zone) EM field would couple to the EUT in free-space. Obtaining answers to these questions are beyond the scope of this contract and are proposed in section 6 as important follow-up work.

2.0 Reverberating/Mode Tuned Chamber Theory of Operation

A reverberating/mode tuned chamber is a large (in terms of wavelength) cavity whose boundary conditions are continuously and randomly perturbed by means of a rotating conductive tuner or stirrer. The time average field inside such a cavity, when sufficient modes are excited, is assumed to be uniform (in level) and formed by uniformly distributed plane waves coming from all directions [1,2]. Resonant modes can exist in the cavity when any of the waveguide modes appropriate to the cavity cross section are a multiple of a half wavelength of the cavity length. The expression for calculating the frequencies of the cavity modes is given as:

$$f_{mnp} = \frac{c}{2} \sqrt{\left(\frac{m}{a}\right)^2 + \left(\frac{n}{b}\right)^2 + \left(\frac{p}{d}\right)^2} \quad (1)$$

where c is the speed of light = 3×10^8 meters/sec, m, n and p are integers representing mode numbers, and a, b, and d are the cavity dimensions in meters.

Dimensions for the TEMEC chamber are shown in figure 1. Table 1 gives the frequencies for the first few modes up to approximately 125 MHz.

Inside a reverberating chamber, the EM field can be characterized by a succession of independent steady state fields that are excited by the long wire transmitting antenna and stirred or tuned by a metal tuner shown in the photograph of figure 2.

The efficiency with which energy can be injected into the chamber is determined by the VSWR or impedance match between the rf source and the transmitting antenna, and by the

ability of the transmitting antenna to couple energy into the particular modes at the appropriate frequencies. This coupling is enhanced by the low-directivity characteristic of the antenna and by the tuner's ability to change the chamber boundary conditions, and hence, shift the mode frequencies to coincide with the source excitation frequency. A simple way to explain the tuner influence is by the graphical interpretation for a rectangular two-dimensional TE case shown in figure 3 [3]. The basic resonance equation is given as

$$k_x^2 + k_y^2 = k_{mn}^2 = \left(\frac{m\pi}{a}\right)^2 + \left(\frac{n\pi}{b}\right)^2 \quad (2)$$

where m and n are mode numbers, a and b are cavity dimensions, in meters, and k's are the wave numbers.

Figure 3 gives the modes intercepted for particular frequencies (or wavelengths) determined by $k_{mn} = \frac{2\pi}{\lambda_{mn}}$. The modes can be shifted, depending upon the Q factor of the chamber and the geometry of the tuner, as indicated by the shaded area. The relationship for determining the boundaries for this area is given as

$$k_{mn} \left(1 - \frac{1}{2Q}\right) < \sqrt{\left(\frac{m\pi}{a}\right)^2 + \left(\frac{n\pi}{b}\right)^2} > k_{mn} \left(1 + \frac{1}{2Q}\right) \quad (3)$$

Of course, not all modes in the shaded area (figure 3) will be present, but only those modes which are excited by the source transmit antenna. Also, not all modes that are excited will be influenced by the tuner, but only those which are influenced by its motion.

The efficiency with which power is received by the receiving antenna is influenced by a number of factors in addition to those mentioned above. These include power loss in the chamber walls, power leakage from the chamber, and the coupling characteristics of the receiving antenna relative to the existing modes in the chamber. The ability to measure the power available at the receiving antenna is also influenced by the receiving antenna and power detector VSWRs (i.e., the impedance mismatch that occurs between the two).

Obviously, if the excitation frequency is high enough, the modal density (number of modes in the shaded area) is so large that omnidirectional, uniform fields, averaged over all tuner positions, can be achieved inside the chamber, even with a small tuner. In such a condition, directivity characteristics of the transmit and/or receive (reference) antenna are washed out and the antennas appear as if they were omnidirectional at these frequencies (for example above 1-2 GHz for a chamber the size of the TEMEC). Continuous modal coverage (at least one mode for each tuner position) is obtained. One would expect field uniformities (time averaged) of better than ± 2 dB. If the number of modes is large, N can be calculated from the expression [4].

$$N \approx \frac{4\pi}{3} \frac{V}{\lambda^3} \quad (4)$$

and the mode density is given by

$$\frac{dN}{df} \approx \frac{4\pi}{f} \frac{V}{\lambda^3} = \frac{3N}{f} \quad (5)$$

V is the cavity volume in equations (4) and (5).

For the TEMEC chamber, $V = 56.7 \text{ m}^3$. At 1 GHz there could be as many as 8796 modes with a mode density of 26×10^{-6} . This means that if the tuner could shift the chamber's modal characteristics equivalent to a frequency shift of 1 MHz at 1 GHz, twenty-six modes could be influenced, (i.e., $\Delta N \approx 26$). In comparison, at 200 MHz, only approximately 70 modes can exist with a mode density of 1.06×10^{-6} . This means that if the tuner could shift the chamber's modal characteristics equivalent to a frequency shift of 1 MHz at 200 MHz, only one mode would be influenced (i.e., $\Delta N \approx 1$).

At lower frequencies (e.g., below 1-2 GHz for the TEMEC) continuous modal coverage is not achieved and the directional characteristics of the particular modes excited start to become apparent. This means that only some EM waves coming from fixed directions are present. Hence, there is a need to design a tuner with three-dimensional tuning characteristics, such as the tuner employed in the TEMEC facility. Also, the transmitting antenna must have omnidirectional properties as much as possible. Again, the long wire antenna used in the TEMEC chamber appears to give satisfactory performance. An additional way to enhance the low frequency modal coverage is to lower the Q of the chamber by increasing chamber loss or leakage. From cavity theory, the Q of a chamber or cavity is given as [5]:

$$Q = \frac{V}{S\delta} \quad (6)$$

where V is the cavity volume in meter³, S is the cavity internal surface area in meters², and δ is skin depth = $\sqrt{\frac{2}{\omega\mu\sigma}}$.

This expression must be considered a maximum or upper bound for a chamber because it assumes the chamber losses are due only to finite wall conductivity.

For most chambers, significant loss occurs from leakage as well as from finite conductivity in the enclosure walls; hence, a more meaningful determination of the average Q, (Q'), can be obtained from measuring the chamber's insertion loss [6]. Insertion loss is defined as the ratio of the power radiated from the chamber transmitting antenna, P_t , to the power received by the chambers reference antenna, P_r .

Assuming uniform energy distribution over the volume of the cavity, the expression for Q' is then:

$$Q' = 16\pi^2 \frac{V}{\lambda^3} \frac{P_r}{P_t} \quad (7)$$

If we assume continuous modal coverage, as required for eq. (7) to be valid, the bandwidth of each mode must be larger than the modal distance (separation in frequency between modes) or

$$\frac{f}{Q} > \frac{df}{dN} \approx \frac{f\lambda^3}{4\pi V} \cdot \quad (8)$$

If Q is large for a particular chamber, the bandwidth of the modes will be small and

continuous modal coverage will be obtained, only if frequency is sufficiently high. For example, insertion loss for the TEMEC chamber is very small indicating a high Q, hence, continuous modal coverage is not obtained, as indicated by the results discussed in section 4, at frequencies below (200-300) MHz.

3.0 Description of TEMEC Measurement Setup and Procedure and NBS Evaluation System

The basic TEMEC susceptibility measurement system is shown in figure 4 [7]. The EUT may be placed anywhere convenient within the chamber provided no point on the EUT is closer than one meter to any wall, the floor, or ceiling. Test, power, and control cables are routed to appropriate monitors, etc., outside the enclosure via filtered feedthrough as required to prevent leakage of fields to the outside environment. The susceptibility test fields are generated inside the enclosure by coupling rf power to the transmitting antenna from an rf source. The electric field strength, E_A , is determined by measuring the pickup power on the receiving antenna through one complete rotation of the field tuner/stirrer for a signal generator power large enough to provide sufficient measurement sensitivity. The received power, P'_r , is sampled while the tuner/stirrer is rotating a minimum of 100 times and the average and peak power are determined.

The power density, P_D , measured in free space using an impedance matched, lossless, receiving antenna is given by [8]

$$P_D = \frac{P_r}{A_R} = \frac{4\pi P_r}{G\lambda^2} \text{ watts/m}^2 \quad (9)$$

where A_R (the effective aperture of the receiving antenna) = $\frac{G\lambda^2}{4\pi}$, G is the antenna gain, and λ is the wavelength in meters. If the receiving antenna is subjected to a plane wave in free space at a sufficient number of different aspect angles, an antenna power pattern can be obtained from which the average response may be determined. The average gain over 4π solid angle is unity and hence eq. (9) can be rewritten in terms of average quantities as:

$$\bar{P}_D = \frac{4\pi \bar{P}_r}{\lambda^2} \text{ watts/m}^2 \quad (10)$$

where \bar{P}_r is the average received power over a 4π solid angle.

In the mode-stirred chamber case, a similar relationship exists if the field distribution at each point in the antenna aperture plane is assumed to be a composite of randomly polarized plane waves. This implies, of course, that the orientation of the receiving antenna will not influence the measured response and hence the effective gain of the antenna is unity.

For the mode-stirred chamber, the "equivalent" average power density is given as [8]

$$\bar{P}'_D = \frac{4\pi \bar{P}'_r}{\lambda^2} \text{ watts/m}^2 \quad (11)$$

where \bar{P}'_r is the average received power in the chamber determined from the receiving antenna response, P'_r , at a sufficient number of different mode tuner positions.

A peak or maximum response can also be determined from the set of measurements resulting from the different mode tuner positions. It is interesting to compare the peak response or peak power density as well as the average power density as a function of location inside the chamber for a fixed input power to the chamber. This may be important because an EUT may respond to the peak of the exposure field as opposed to the "average" field.

In performing susceptibility tests, the input power, P_{in} , is adjusted as required to obtain the test level power density desired as determined from eq. (11), and the measurement of \bar{P}'_r with the EUT in place. The equivalent electric field, E_A , is then found by using the expression:

$$E_A = \sqrt{\eta \bar{P}'_D} = \frac{4\pi}{\lambda} \sqrt{30 \bar{P}'_r} \quad (12)$$

where η is the intrinsic wave impedance in the chamber. Equation (12) assumes planar far-field conditions. Obviously, such conditions do not exist inside a multimoded chamber; hence, the equation's validity is questionable. However, since data to determine E_A is statistically averaged from a set of measurements made at many different tuner positions over a complete rotation of the tuner, using an average value of 120π ohms for the wave impedance may be reasonable.

One of the major objectives of this evaluation program (as stated earlier) was to experimentally determine the validity of eq. (12) (i.e., the absolute amplitude calibration accuracy of the test fields in the chamber). To accomplish this, the TEMEC test system was modified slightly by NBS for evaluation purposes. A block diagram of the modified system is shown in figure 5. The purpose of using a calibrated bidirectional coupler is to measure the net power flow to the transmit antenna as opposed to measuring only the incident power. This allows corrections to be made for changes in the net input power resulting from antenna-rf generator impedance mismatch and rf generator output variations that occur during a complete rotation of the field tuner. The bidirectional coupler was also used to evaluate the VSWR of both the transmit and reference antennas. This was achieved by measuring the return loss from the antennas when rf power was applied at their input/output terminals through the coupler.

A precision 10 dB attenuator and power detector were used in place of the calibrated receiver to measure the receiving antenna power. This was done to minimize impedance mismatch with the receiving antenna.

Mapping of the field distribution and determination of the absolute field levels were made using the NBS calibrated isotropic E-field probe [9] and scanning system shown in figure 6. The system is made of dielectric material and is designed for a minimum perturbation/interaction with the test fields established in the chamber. The field probe for evaluating the chamber serves as a standard EUT and causes minimal perturbation of the test field.

4.0 TEMEC Analysis/Evaluation Results

4.1 Transmit and Receive Antennas VSWR

VSWR measurements were performed to determine potential error resulting from changes in net input power occurring during a complete rotation cycle of the tuner. These measurements were also made for the transmitting antenna and receiving antenna as a function of frequency for a fixed tuner position. Results of these measurements are shown in figures 7 and 8. The long wire transmitting antenna maximum VSWR is high (35:1) at 100 MHz but decreases substantially as the frequency increases. In contrast the maximum VSWR of the receiving antenna remains high (>10:1) over the measured frequency range of 200 MHz to 1.0 GHz.

The received power available at the antenna terminal was measured using a 10 dB precision attenuator and power detector with a combination VSWR shown in figure 9. If actual power delivered to the load (power meter) is to be compared with the maximum available from the source (receiving antenna), a conjugate impedance match must exist.

Power transfer between a source and a load of reflection coefficients Γ_S and Γ_L is given as

$$P_f = \frac{\text{fraction of maximum available power absorbed by the load}}{\text{by the load}} = \frac{(1 - |\Gamma_S|^2)(1 - |\Gamma_L|^2)}{|1 - \Gamma_S \Gamma_L|^2} \quad (13)$$

where Γ_S and Γ_L denote reflection coefficient magnitude and phase.

$|\Gamma_S|$ and $|\Gamma_L|$ can be obtained from the appropriate VSWR by the expressions

$$|\Gamma_S| = \frac{\text{VSWR} - 1}{\text{VSWR} + 1}.$$

If the load (power detector) VSWR is 1.065 (worst case) and the receiving antenna (source VSWR) is as great as 10.0,

$$|\Gamma_S| = \frac{10 - 1}{10 + 1} = .8182, \quad |\Gamma_L| = \frac{1.065 - 1}{1.065 + 1} = .0315$$

$$P_{F_{\min}} = .3219 = -4.92 \text{ dB}$$

$$P_{F_{\max}} = .3479 = -4.59 \text{ dB}$$

or an error as large as -4.92 dB could exist in the measurement of the receiving antenna power. Obviously this error could be reduced, at least at frequencies above 300 MHz, if the receiving antenna VSWR was improved to be comparable with the transmitting antenna. Considerable error can also exist, as mentioned earlier, in the determination of the chamber test field level if the net input power is assumed constant during a complete revolution of the tuner. The normal calibration procedure appears to make this assumption. This error is discussed in more detail in section 4.4.

4.2 Chamber Coupling Efficiency/Insertion Loss

The chamber coupling efficiency or loss was determined at a number of discrete frequencies as shown in figure 10. These data were obtained at each frequency by measuring the net input power ($P_{\text{incident}} - P_{\text{reflected}}$) to the transmitting antenna, and by measuring the receiving antenna power, for 100 stepped positions equal to one full rotation of the tuner. Changes in the net input power were normalized to give a receiving antenna output proportional to a constant net input power. These data for the minimum and average insertion losses are shown as the solid curves in figure 10. The dashed curves show the minimum and average losses determined without normalization or correction for net input power changes. It is interesting to note that even though large point by point differences occur between the normalized and raw data, statistically the raw and normalized data minimums and average loss values agree quite well.

4.3 Test Zone E-Field Uniformity

E-field uniformity in the test zone of the TEMEC chamber was evaluated as a function of position along two orthogonal scans using the measurement system shown in figure 11. Location of the two scans are shown in figure 12. Measurements were made of each orthogonal component of the E-field ($E_V = \text{vertical}$, $E_T = \text{transverse}$, and $E_L = \text{longitudinal}$) and the hermitian magnitude, $E_p = \sqrt{E_V^2 + E_T^2 + E_L^2}$. Measurement results obtained along the transverse scan (across the width of the chamber), at 5 frequencies are given in figure 13. These data were obtained by measuring the maximum E-field components and magnitude at (5-10) cm increments in position along the 2 meter scan. No attempt was made to normalize these measurements to correct for net input power changes as a function of tuner or probe position. The minimum of the E-field magnitude, $E_{p_{\text{min}}}$, at 500 MHz and 700 MHz is also given. At 1000 MHz, only E_p maximum is given. Notice that as the frequency increases, the variation in $E_{p_{\text{max}}}$ with position decreases. The measurement results are summarized in Tables 2 & 3. The difference between $E_{V_{\text{max}}}$, $E_{T_{\text{max}}}$, $E_{L_{\text{max}}}$, and $E_{p_{\text{max}}}$ (shown in Table 3) indicates the chamber discrimination to EUT radiation directivity and polarization. Recall that if sufficient modes or mode tuning exists, the chamber will couple the EUT radiation independent of its polarization. Obviously, this is not happening at the lower frequencies but is becoming less polarization dependent as the frequency increases. An analysis of the data of figure 13, especially at 200 MHz, gives some indication of which modes exist inside the chamber. The relationship between $E_{p_{\text{max}}}$ and $E_{p_{\text{min}}}$ in figure 13c and 13d is also worth noting. At 200 and 300 MHz, the $E_{p_{\text{min}}}$ was less than the resolution of the probe and instrumentation. This indicates the tuner capability to influence the amplitude of the excited modes at positions along the scan. As the frequency increases, the number of modes excited increases rapidly and the tuner has more effect on coupling the fields to the probe (EUT). Recall from section 2 that at frequencies for which continuous modal coverage exists, minimal tuning is required. At these frequencies (above approximately - 2 GHz) $E_{p_{\text{min}}}$ will approach $E_{p_{\text{max}}}$ in amplitude and the

time averaged field variations with position will approach zero.

E-field measurements were also made along longitudinal scans (along the length of the chamber) indicated in figure 12. These results, shown in figure 14, give the variations in $E_{p_{max}}$ with measurement position for 100 MHz, 200 MHz and 300 MHz. The mode characteristic at 100 MHz is very evident. Again, these data were not corrected for changes in net input power that occur as a function of tuner position and probe location.

Figure 15 gives the results of measurements made at 200 MHz using the computer based system (figure 5) to correct for variations in the net input power. Results are given for both the maximum E_p and the average E_p as a function of position. The maximum E_p can be compared to figure 14 to give an indication of errors that exist (at 200 MHz) due to failure to correct for input power variations. An estimate of the error anticipated by failure to normalize the measurements of E_p and E_A to an equivalent constant net input power can be obtained from figures 16 and 17 and the results are summarized in Table 4.

4.4 E-Field Amplitude Calibration

Measurements were made to determine the absolute amplitude of the E-field inside the TEMEC chamber relative to planar E-field calibrations. The NBS probe used to make these measurements was calibrated using a TEM cell [10] and anechoic chamber to determine its output response as a function of absolute E-field (far-field) level at the calibration frequencies. The probe was placed at the center of the TEMEC test chamber with all three channels operating to give an isotropic response to the field. This measured E-field amplitude, E_p , was then compared to the E-field amplitude, E_A , determined from a simultaneous measurement made of the power available at the terminals of the receiving antenna and calculated from eq. (11). The results of these measurements as a function of tuner position are shown in figures 16 and 17. The solid curves gives the E-field corrected for net input power variations (i.e., the probe and receiving antenna output response were adjusted to give the equivalent for a constant (normalized) net input power.) The dashed curves are the results obtained from raw data (i.e., before a correction was applied for net input power variations). The maximum and average E-field values obtained from the data shown in figures 16 and 17 are summarized in the graphs of figure 18. The differences in the E-field as determined from the probe measurements and the receiving antenna received power measurements are summarized in Table 5.

The accuracy of these results is dependent on the ability to determine E_p and E_A from their appropriate measurements and computations. The calibration accuracy for the probe E-field measurements is estimated at approximately ± 1 dB [9]. The uncertainty in the E-field determination based on measuring the maximum and average available power from the receiving antenna is difficult to estimate. This uncertainty is caused by the contribution in the uncertainties of the measurement parameters and the validity of the assumption made in equation (11). The purpose of Table 5, of course, is to provide the basis for estimating the accuracy in E_A by comparing E_A with the calibration probe field measurement.

It is interesting to compare the normalized (corrected for input power fluctuations) difference between the measured E-field inside the TEMEC chamber as determined using the NBS probe and the chamber receiving antenna as a function of the NBS probe's position in the chamber. Figure 19 gives an example of the results obtained at 200 MHz for maximum and average E_p and E_A along a longitudinal scan. Note that as the probe moves away from the receiving antenna toward the transmitting antenna, the measured field increases and the difference between E_p and E_A increases.

5.0 Conclusions

The following conclusions can be drawn from the results of the evaluation of the TEMEC chamber.

- (1) Modes are excited and effectively tuned in the chamber at frequencies down to 100 MHz. VSWR of the transmitting antenna is high at low frequencies (approaching 200 MHz and below) but improves rapidly with increasing frequency. This antenna design appears suited for this application. The tuner employed in TEMEC also is effective and appears to work satisfactorily.
- (2) The long wire used as the receiving antenna has a very high VSWR across the test frequency range. This can contribute to large errors (up to 5 dB) in received, available power measurements due to mismatch. It would be preferable to use an antenna similar to the transmitting antenna with improved VSWR characteristics.
- (3) Mode structure is strongly present at 100 MHz (field variation of 15.3 dB in test zone) and at 200 MHz (field variation of 6.5 dB in test zone), but decreases as frequency increases (3.7 dB at 1000 MHz).
- (4) The E-field is also polarization dependent inside at the lower frequencies. This effect is apparent up to at least 700 MHz but is decreasing with frequency (i.e., figure 13 and table 3 indicate average differences between E_p , E_y , E_L , and E_z of approximately 6 dB at 200 MHz to approximately 4 dB at 700 MHz).
- (5) The insertion loss is low; (average loss of 4.5 dB at 100 MHz to 9.5 dB at 1000 MHz, see figure 10) indicating the chamber has a high Q. This will limit modal coverage at lower frequencies where the mode density is small. It may be advisable to increase the chamber loss by a few dB to improve low frequency field uniformity.
- (6) The potential difference in determining maximum and average E-field in the chamber with or without correcting for net input power changes is 4.7 dB at 100 MHz, decreasing to 0.35 dB at 1000 MHz (Table 4) by using the receiving antenna.
- (7) The difference in determining the absolute level of the E-field in the test zone using the NBS calibrated, isotropic probe as compared to using the chamber's receiving antenna is between 3.9 dB - 8.2 dB (Table 5). This corresponds to an apparent average systematic offset error of 6.2 dB (i.e., the measured E-field inside the chamber is

6.2 ± 2.3 dB greater than the E-field calculated from eq. (12) using the chamber's receiving antennas received power measurements). It is important to note this apparent offset error results from a limited set of data for this particular chamber and should not be considered conclusive for application to mode tuned chambers in general. Additional research is needed to substantiate these results at additional frequencies and with other chambers. Some suggested reasons for an offset error, however, include, but are not necessarily limited to:

- a) Errors in measuring the total power available at the chamber's receiving antenna. This can result from the impedance mismatch that exists between the antenna and its power detectors as a function of the chamber's mode-tuner position;
- b) The fact that maximum coupling of power from the source connected to the transmitting antenna, thence to the excited modes in the chamber and thence to the receiving antenna, is not likely to occur all simultaneously for any mode-tuner position; and
- c) Evanescent modes, as well as propagating modes, may exist inside the chamber which may contribute to the total field. Such modes are not included in eq. (11).

The mode tuned concept (TEMEC), using a computer based system for control, data acquisition, and data analysis, is superior to continuous mode stirring. This is apparent due to the ability to monitor and normalize output to input parameters variations and to control test-field variation time constants. The field exposure time constant is important when performing equipment susceptibility tests and must be sufficiently long to allow the EUT time to respond.

The TEMEC facility can be operated as a mode tuned chamber at frequencies down to 100 MHz. Accuracy in establishing the test field level in the chamber as determined by receiving antenna power measurements may be reasonable, assuming a systematic offset correction before inserting an EUT. However, the influence of an EUT on the test field was not determined in this study. This effect could be substantial and should be analyzed before the uncertainty in establishing test fields with the EUT present can be determined (see section 6, Recommendations).

6.0 Recommendations

Results of this study, coupled with other research into the mode tuned/stirred measurement technique, indicate that this technique may have considerable potential for performing EM susceptibility measurements. Unresolved questions, referred to in section 1 of this report, emphasize the need to perform the following tasks.

- (1) Perform measurements to evaluate interactions between the EUT, the test field, and the field generation equipment. This would require measurements to determine the ability

to establish the absolute level of test field in the chamber after insertion of the EUT. These results should be carefully analyzed to determine if a systematic offset error exists as suggested by the results of Table 5 and conclusion 7 of this report, (i.e., if the actual test field is consistently greater than the field calculated from the receiving antenna power measurements).

- (2) Analyze the ability of the enclosure's complex field to couple to the EUT as compared to open-space planar field coupling. This may require measurements of rf currents coupled onto EUT input/output and power line cables and on EUT enclosures.
- (3) Analyze, where feasible, the boundary value problem associated with inserting an EUT inside the enclosure.

7.0 Acknowledgments

Work described in this report was sponsored by the Pacific Missile Test Center, Point Mugu, California, with Mr. Ken Canoga as project monitor. The facility evaluated is located at McDonnell Douglas Astronautic Corp. East, St. Louis, Missouri.

The author wishes to acknowledge the assistance of James Roe and Ed Gardner of McDonnell Douglas Astronautics Company for their assistance and cooperation in performing the measurements discussed in this report. The author further recognizes the benefit of the discussions he had with Dr. Mark T. Ma (NBS) in both developing approaches to evaluate the facility and in analyzing and explaining the results of data obtained. He also appreciates the assistance of Drs. Carl F. Stubenrauch (NBS) and David C. Chang (University of Colorado) in reviewing this report.

8.0 References

- [1] Ramo, S. and Whinney, J. R., *Fields and Waves in Modern Radio*, 2nd ed., (pp 418-428), (Wiley, New York, November 1960).
- [2] Corona, P., Latmiral, G., Paolini, E., and Piccioli, L., Use of a Reverberating Enclosure for Measurements of Radiated Power in the Microwave Range, *IEEE Trans. on EMC EMC-18*, [2] (May 1976).
- [3] Corona, P., Istituto Universitario Navale, Napoli Italy - Private Communication.
- [4] Mendez, H. A., A New Approach to Electromagnetic Field-Strength Measurements in Shielded Enclosures, *Wescon Technical Papers* (1968).
- [5] ArGENCY, E., and Kahan, T., *Theory of Waveguides and Cavity Resonators* (Hart Publishing Co., New York, DATE?).
- [6] Corona, P., Latmiral, G., and Paolini, E., Performance and Analysis of Reverberating Enclosures with Variable Geometry, *IEEE Trans. on EMC EMC-22*, [1], (Feb 1980).
- [7] Cumming, J. R., Translational Electromagnetic Environment Chamber, A New Method for Measuring Radiated Susceptibility and Emissions, *IEEE International Symposium of EMC*, San Antonio, Texas, *IEEE 75 CH 1002-5 EMC* (October 1975).
- [8] Bearn, J.L. and Hall, R.A., "Electromagnetic susceptibility measurements using a mode-stirred chamber," *IEEE International Symp. n EMC*, Atlanta, GA, June 20-22, 1978, 78-CH-1304-5 EMC.
- [9] Bowman, R. R., Larsen, E. B., Belsher, D. R., and Wacker, P. F., Second Progress Report: Electromagnetic Hazards Project, NBS Report, unpublished (September 18, 1970) Private communication.
- [10] Crawford, M. L., Generation of Standard EM Fields for Calibration of Power Density Meters 20 KHz to 1000 MHz, *NBSIR 75-804* (January 1975).

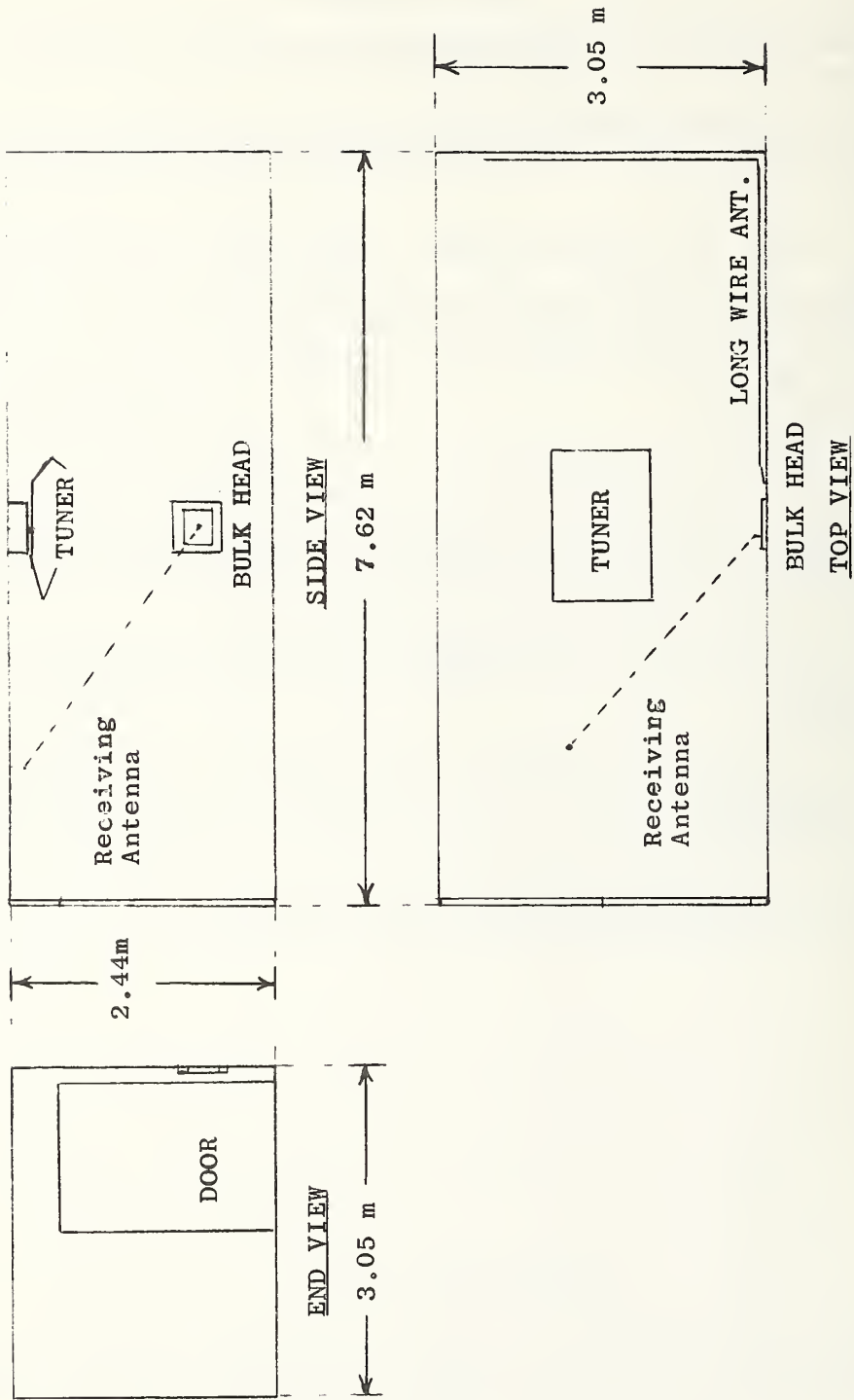


Figure 1. Cross sectional views of TEMEC (Mode Tuned Chamber).



Figure 2. Photograph of field tuner/stirrer installed in 2.4m x 3.0m x 7.6m shielded enclosure.

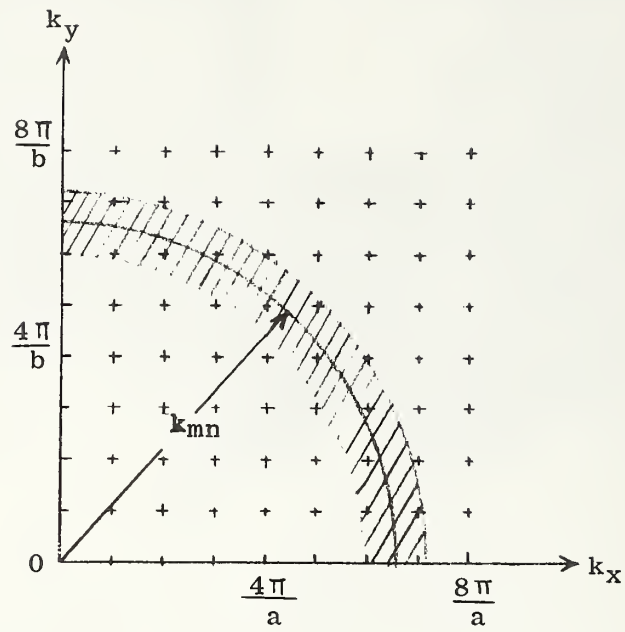


Figure 3. Two dimensional graphic interpretation of modes inside resonant chamber.

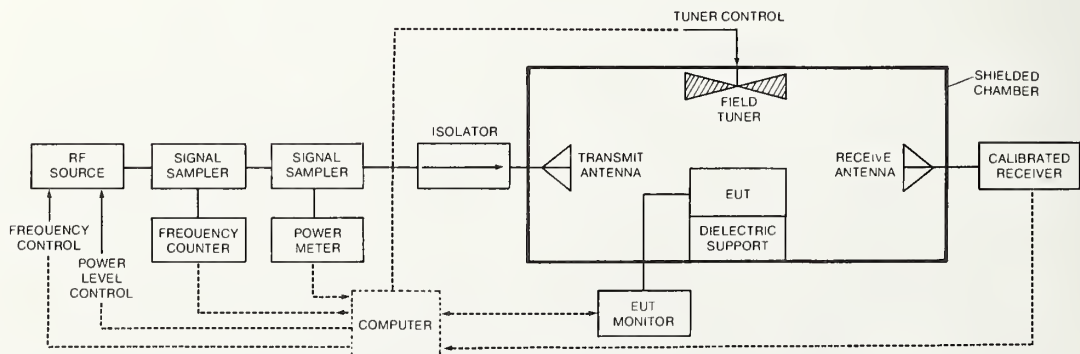


Figure 4. Mode tuned enclosure EMC measurement system.

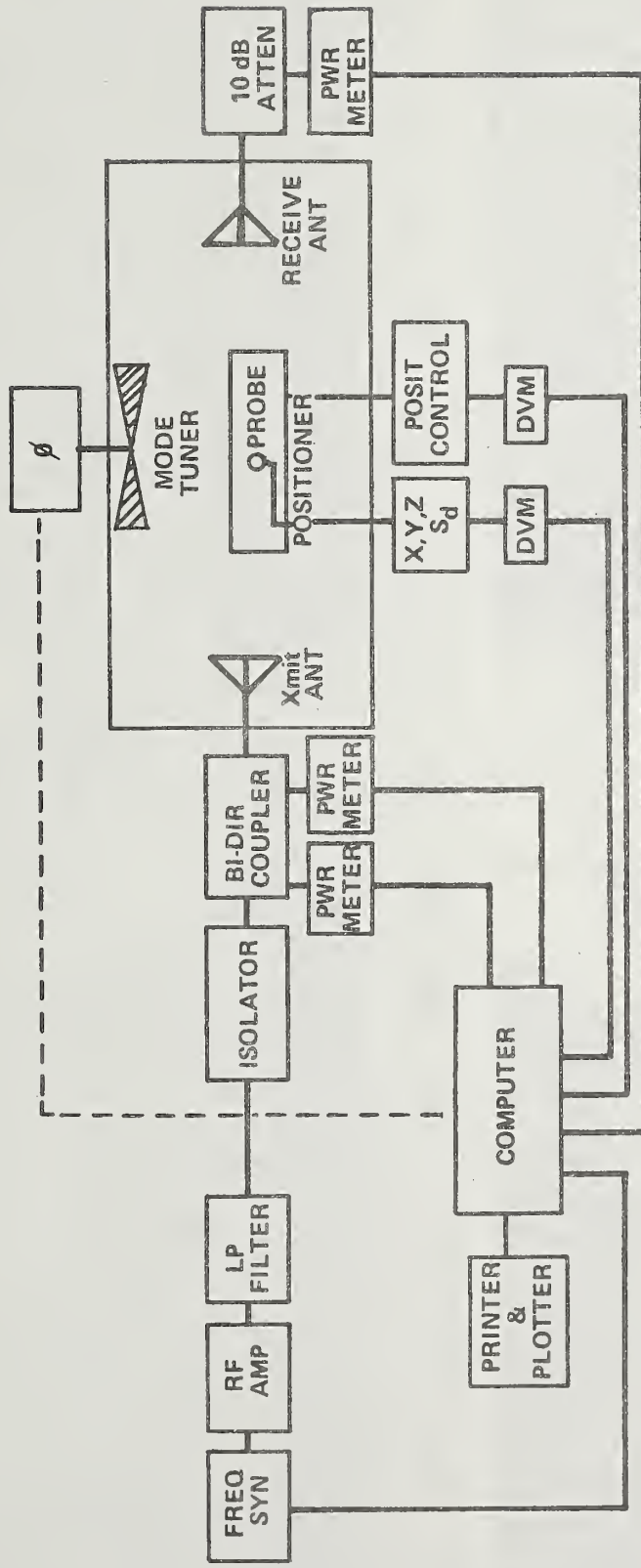


Figure 5. Block diagram of NBS modified mode tuned enclosure evaluation system for EMC measurements.

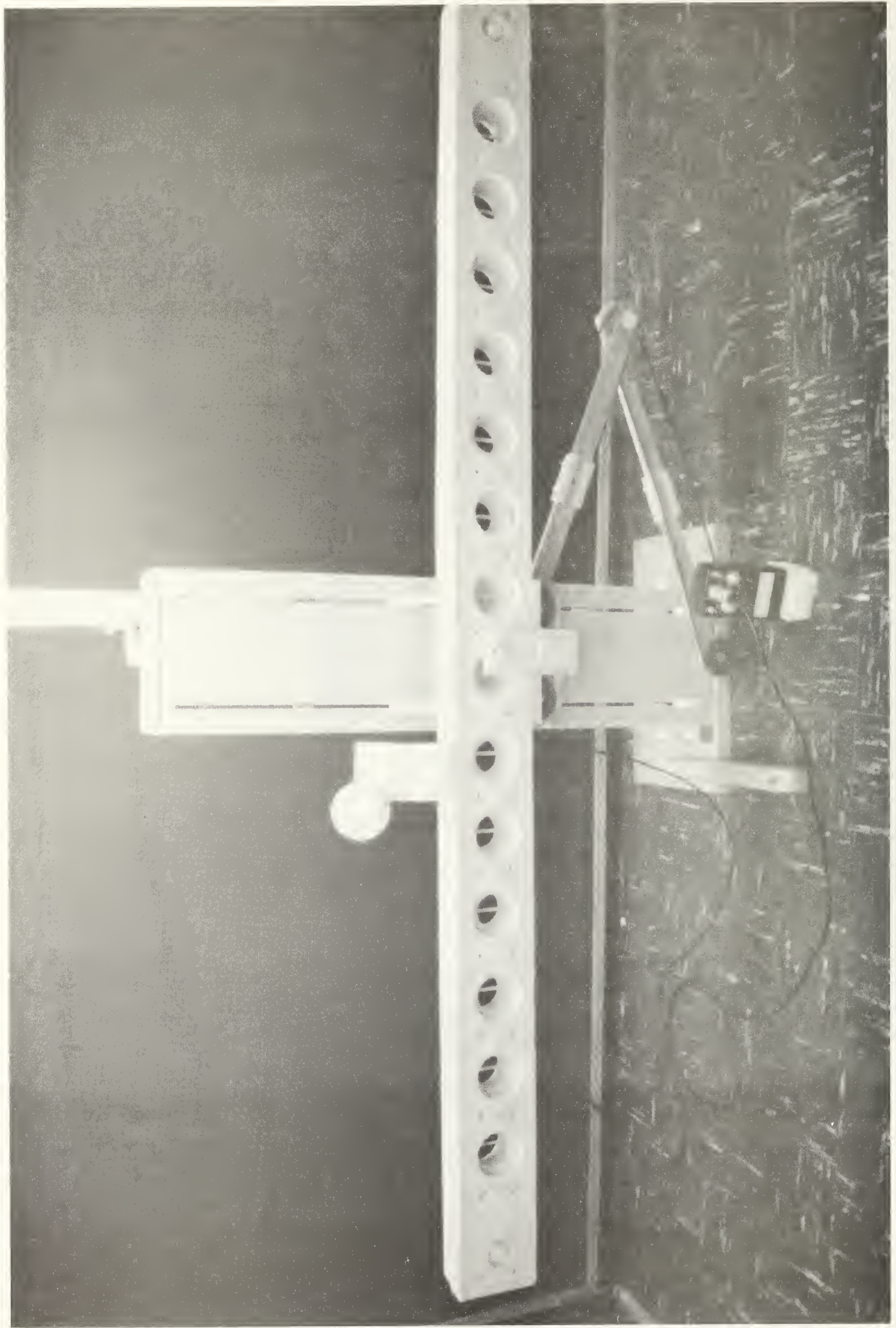


Figure 6. NBS isotropic E-field probe and scanning system.

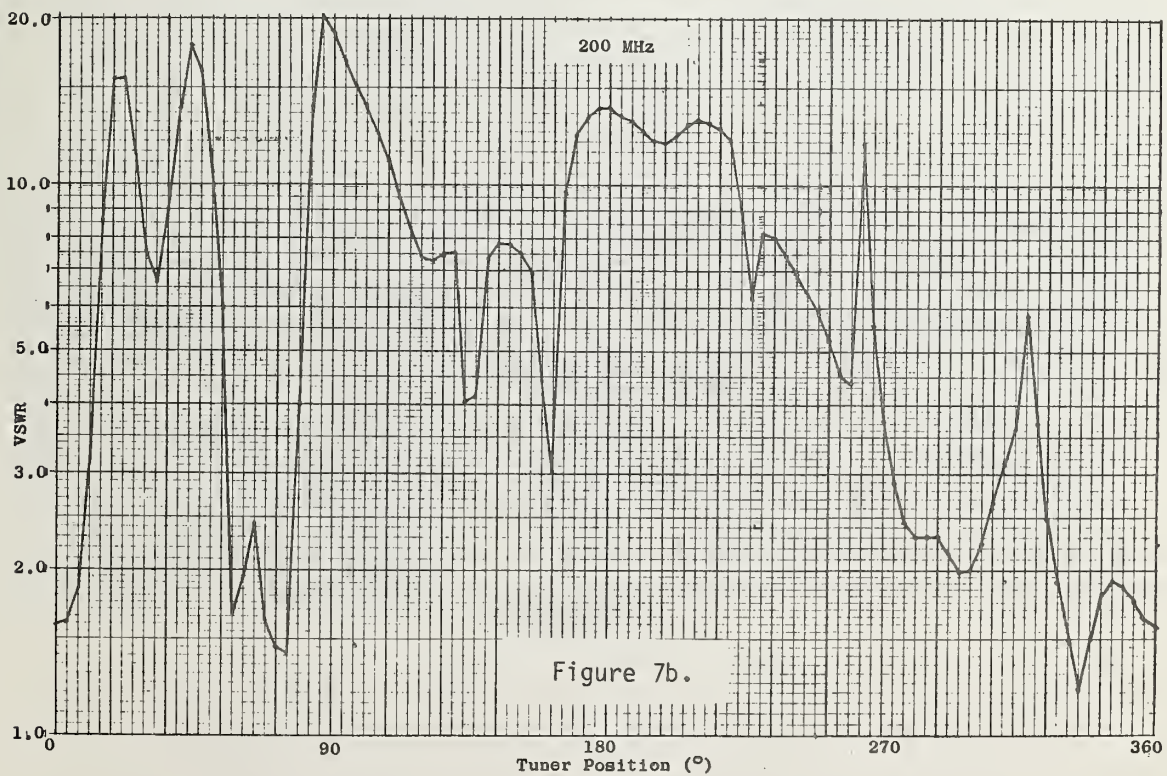
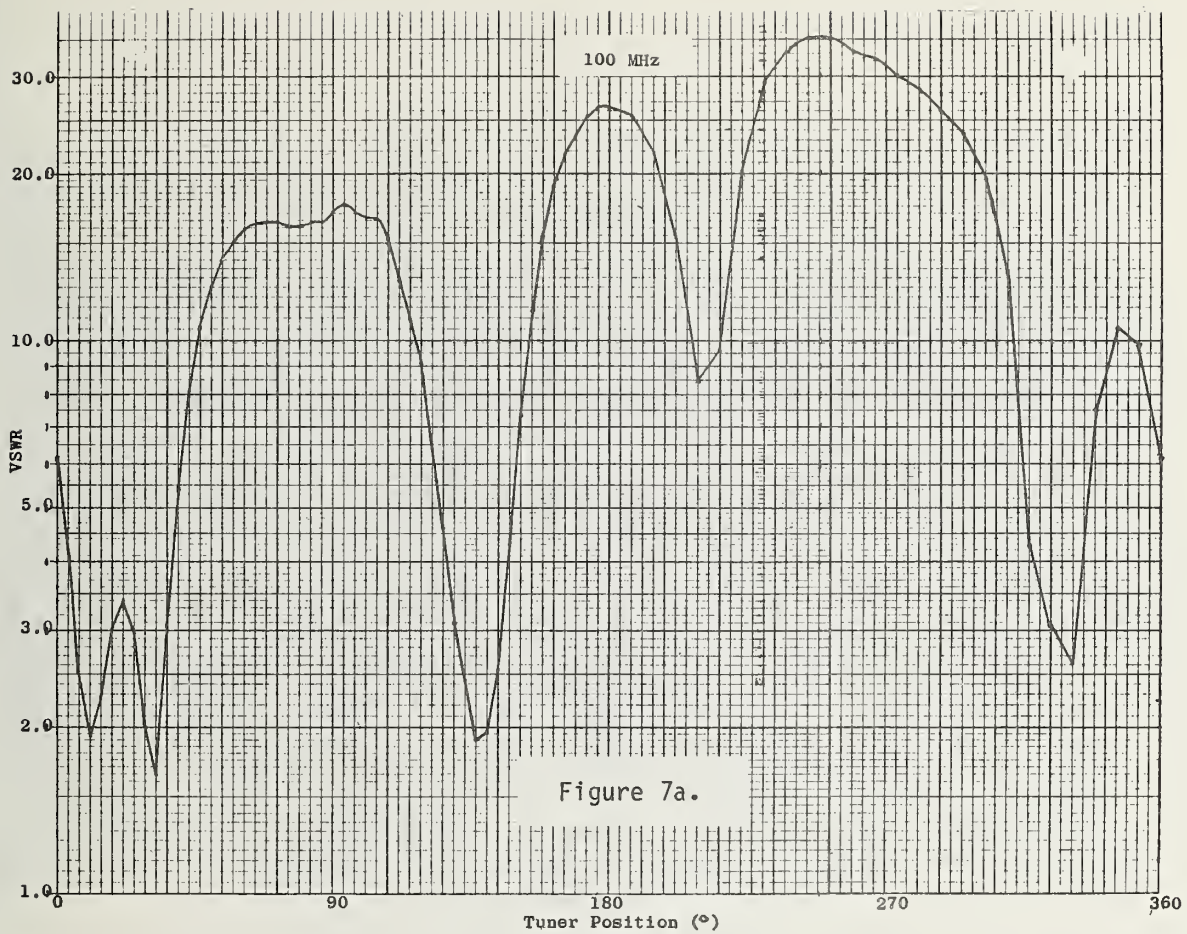
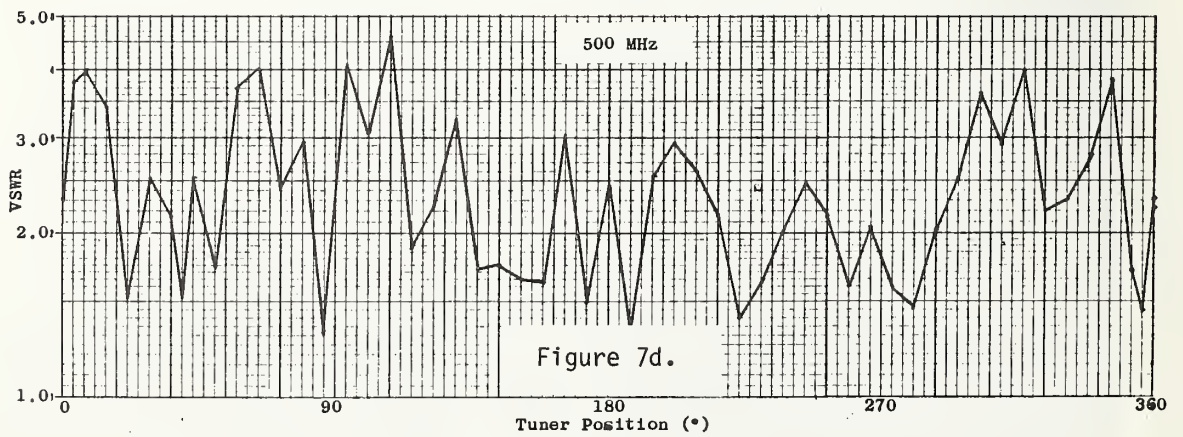
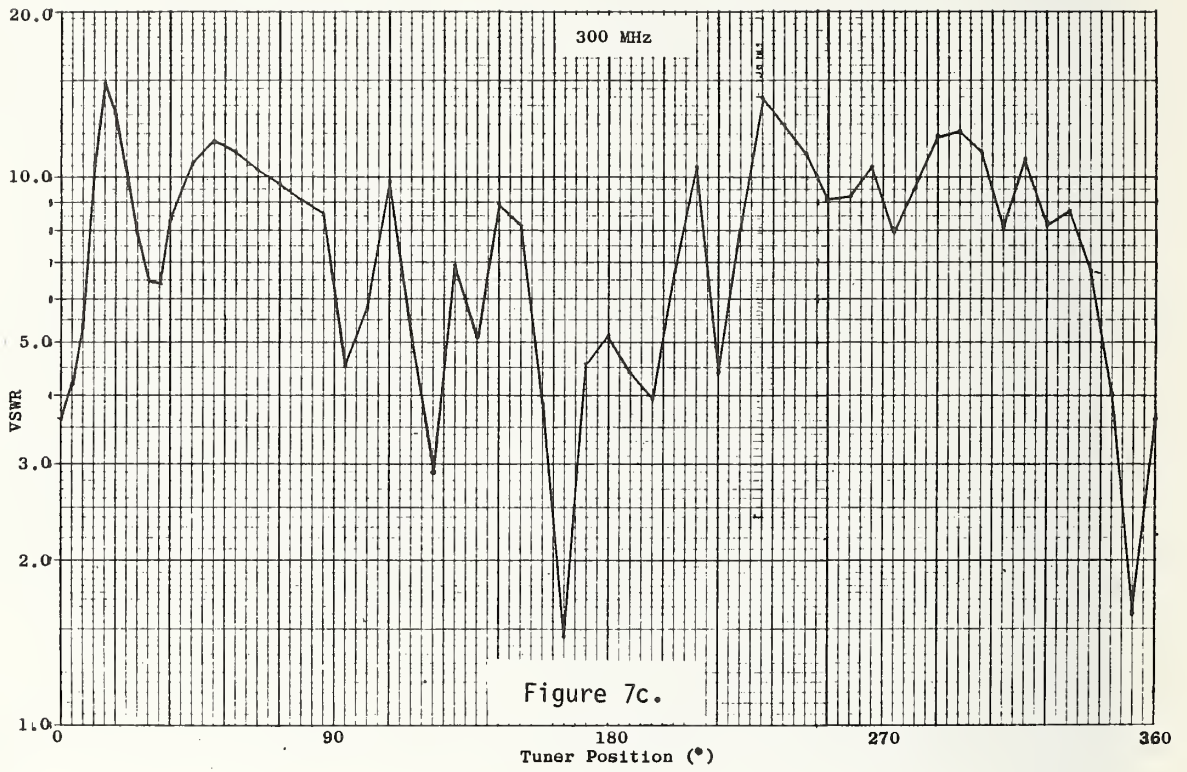
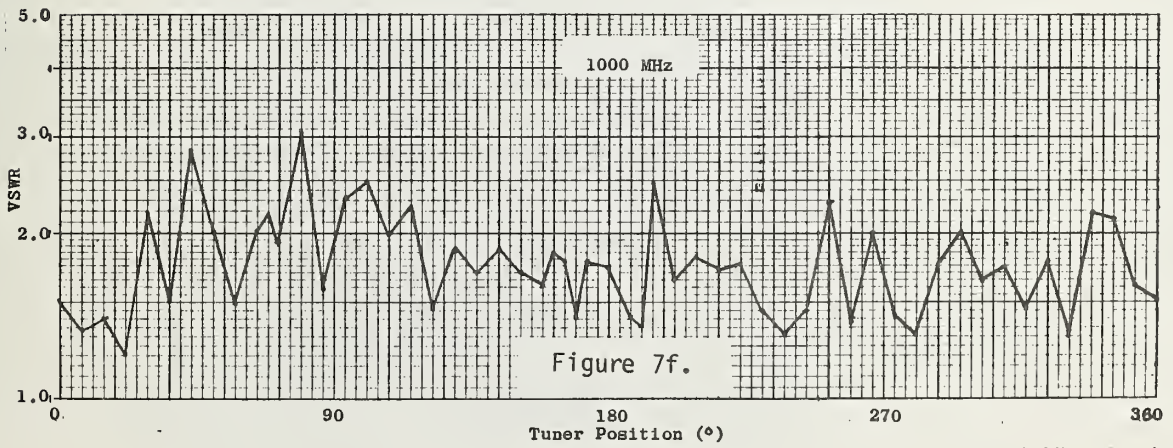
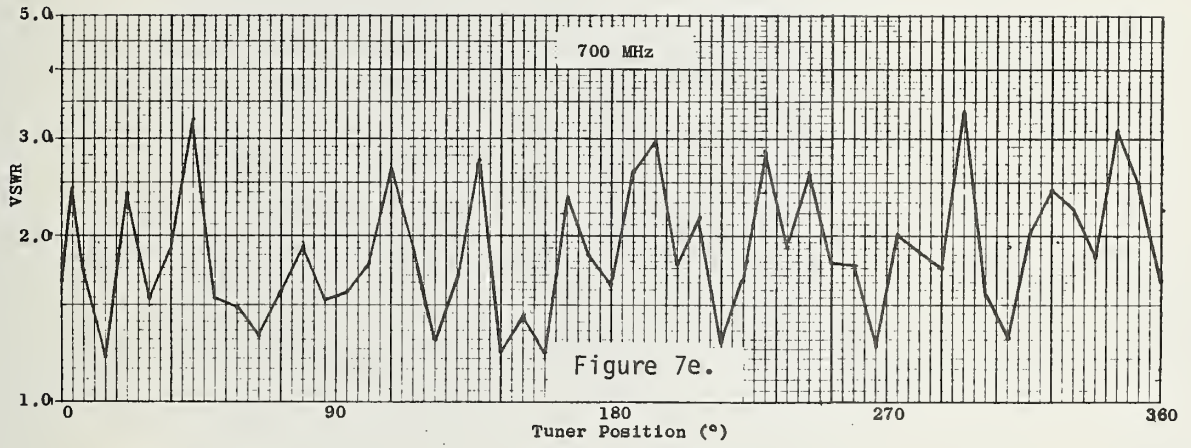


Figure 7. Input VSWR of long wire transmitting antenna as a function of tuner position.





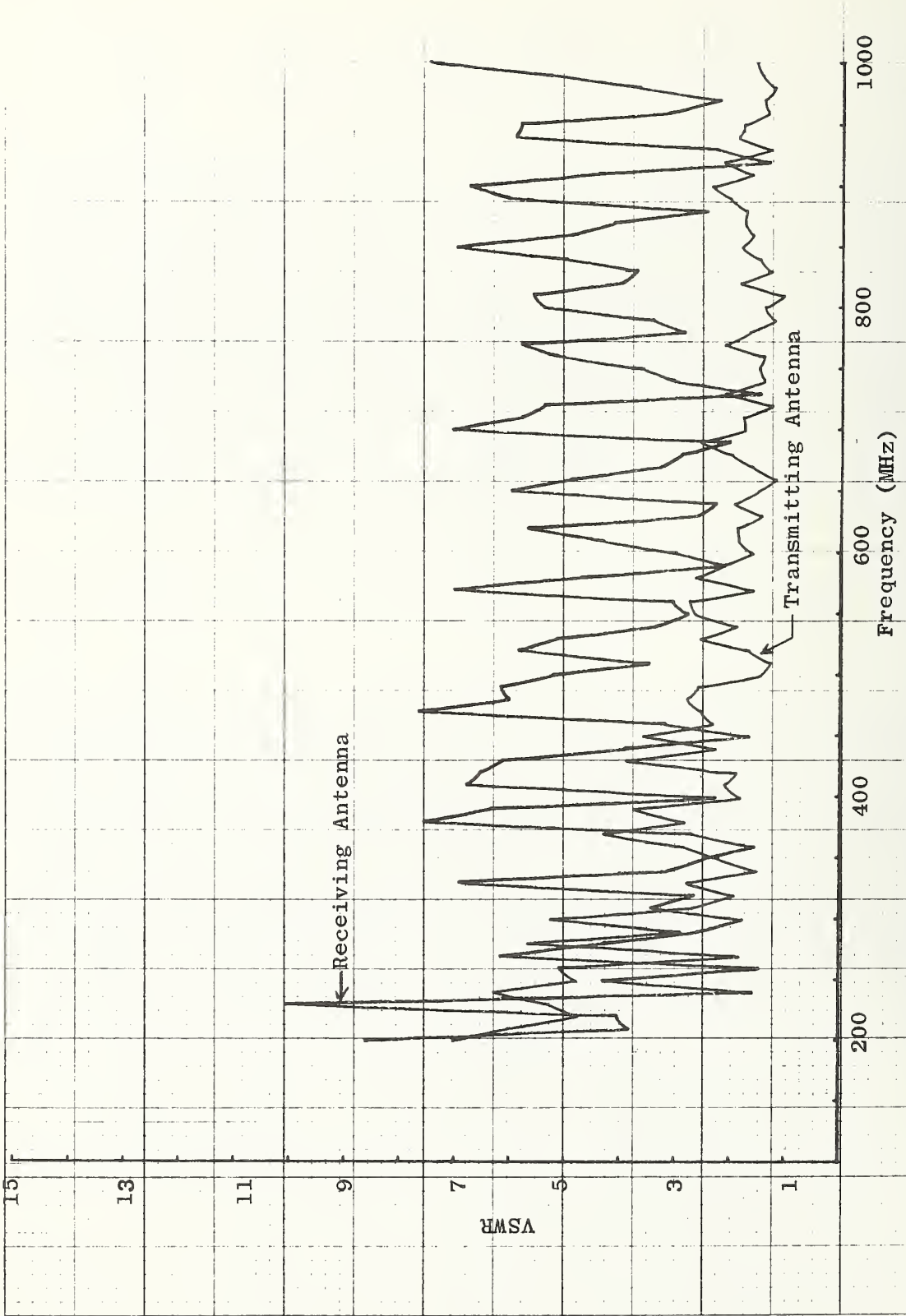


Figure 8. VSWR of transmitting and receiving antennas. Tuner in fixed position.

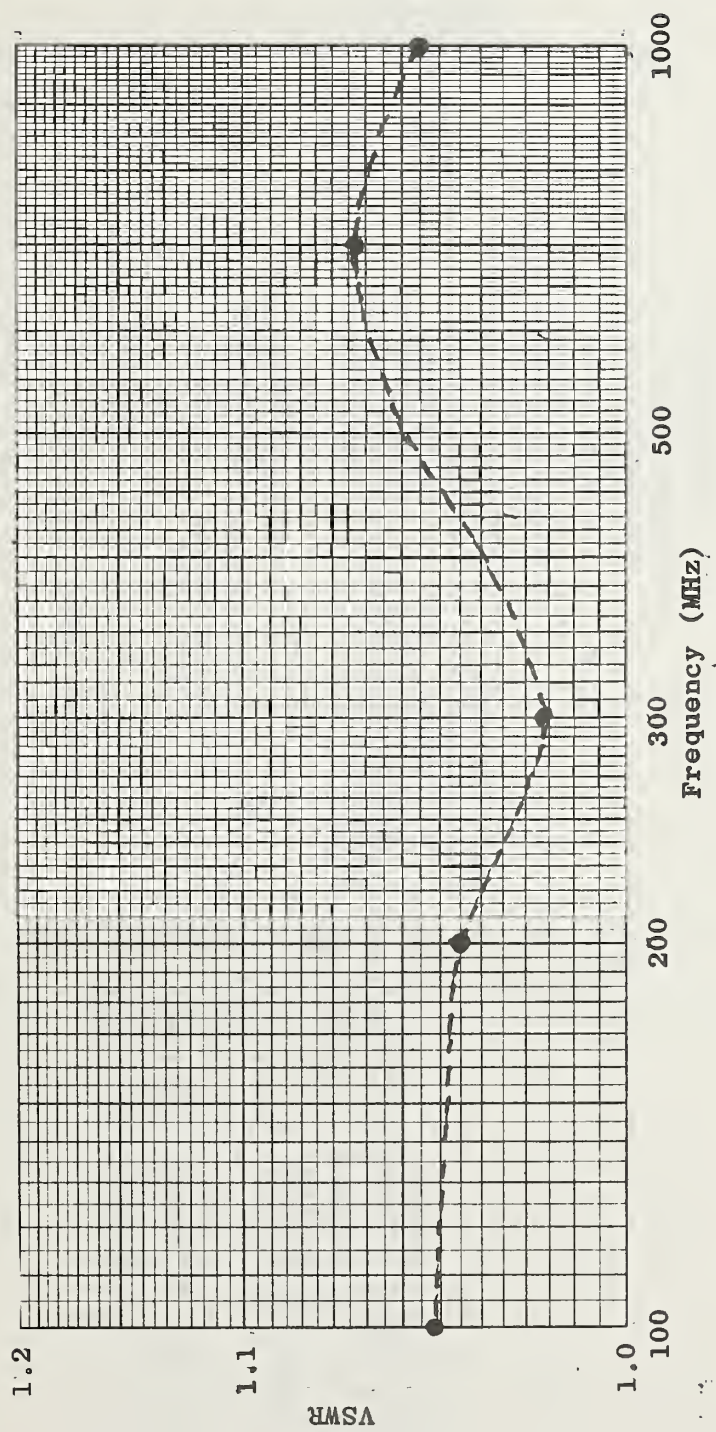


Figure 9. VSWR of 10 dB attenuator-power detector used to measure received power from reference antenna.

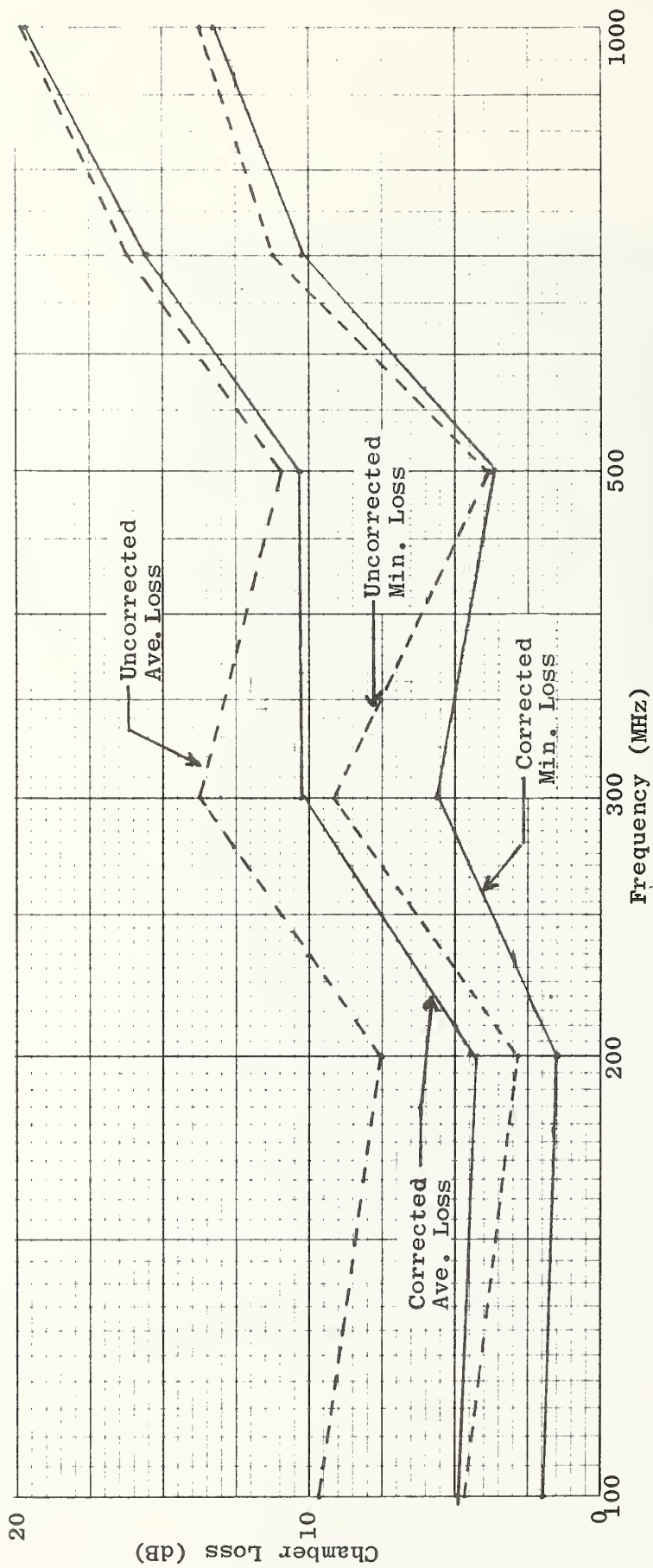


Figure 10. Minimum and average insertion loss of TEMEC (mode tuned chamber) with and without correction for net input power changes. Uncorrected based on incident power. Corrected based on net input power.

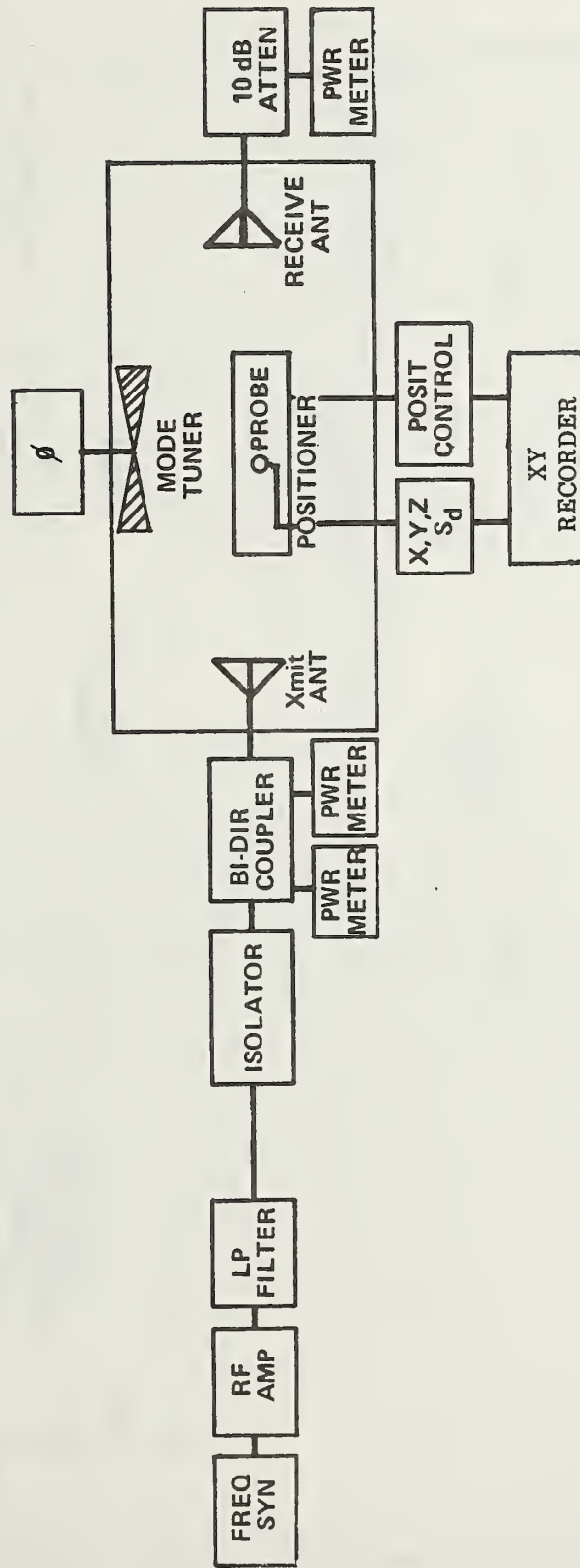


Figure 11. Block diagram of system for evaluating E-field uniformity in test zone of TEMEC.

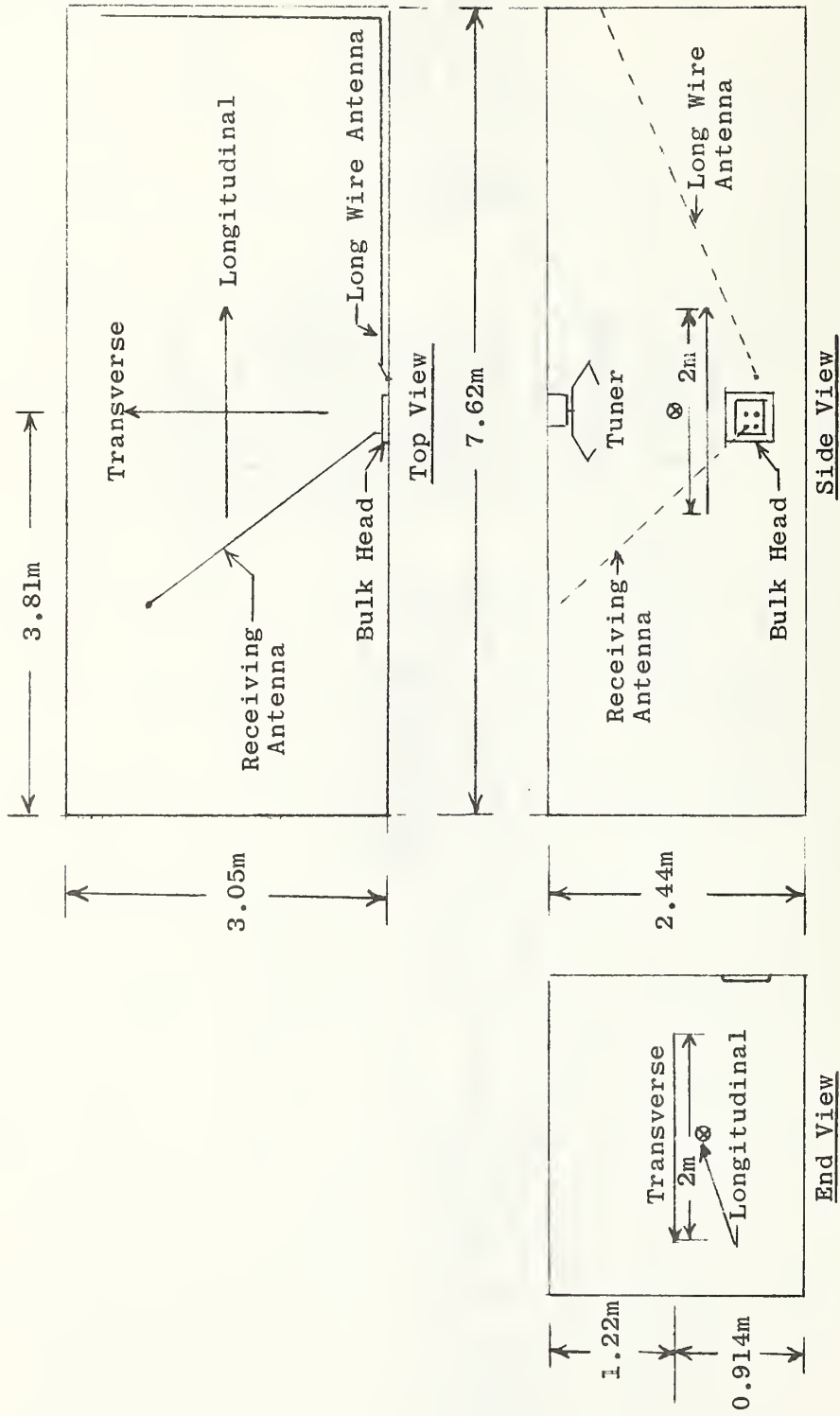


Figure 12. Cross sectional views of TEMEC showing location of transverse and longitudinal scans.

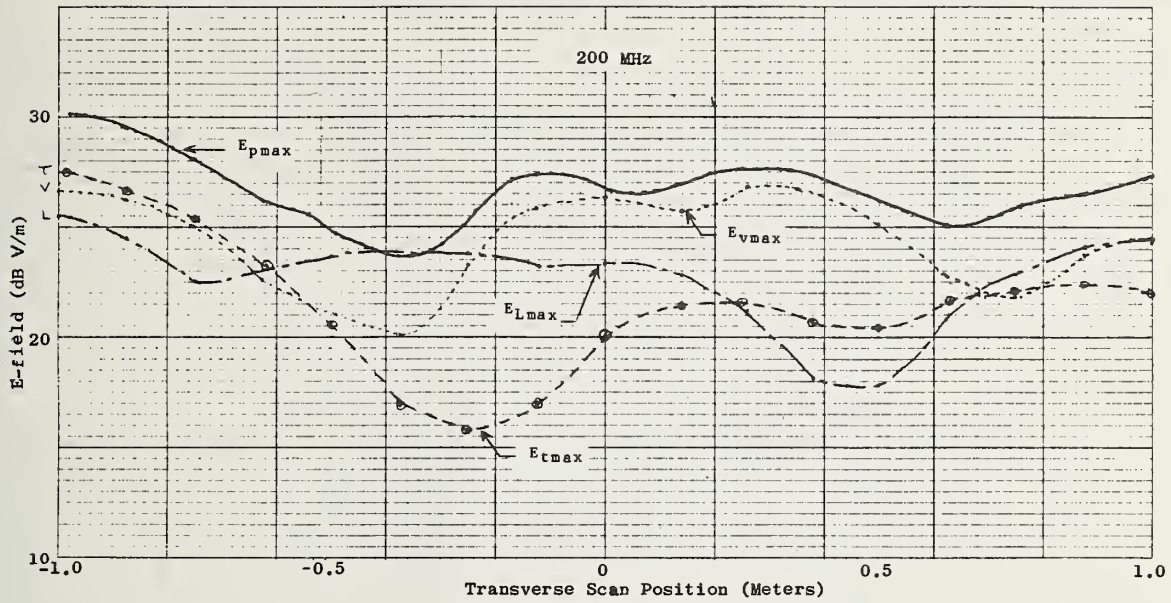


Figure 13a.

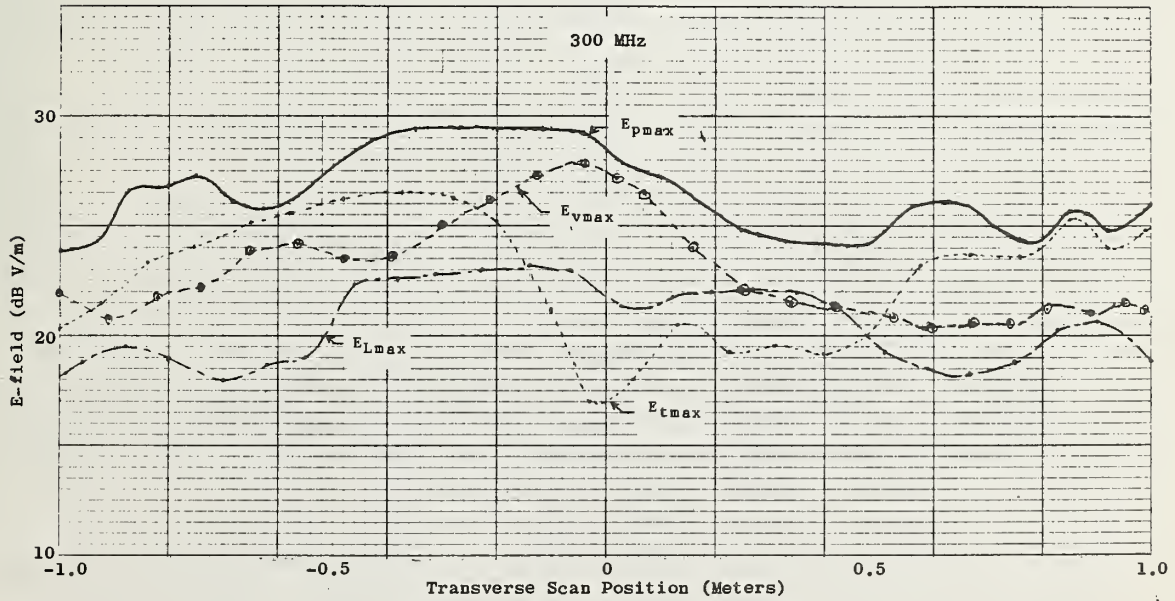


Figure 13b.

Figure 13. Results of E-field uniformity measurements taken along transverse scans through center of TEMEC test zone. Results are maximum amplitudes obtained from measurements made for complete revolution of tuner (unless otherwise indicated) as a function of probe position.

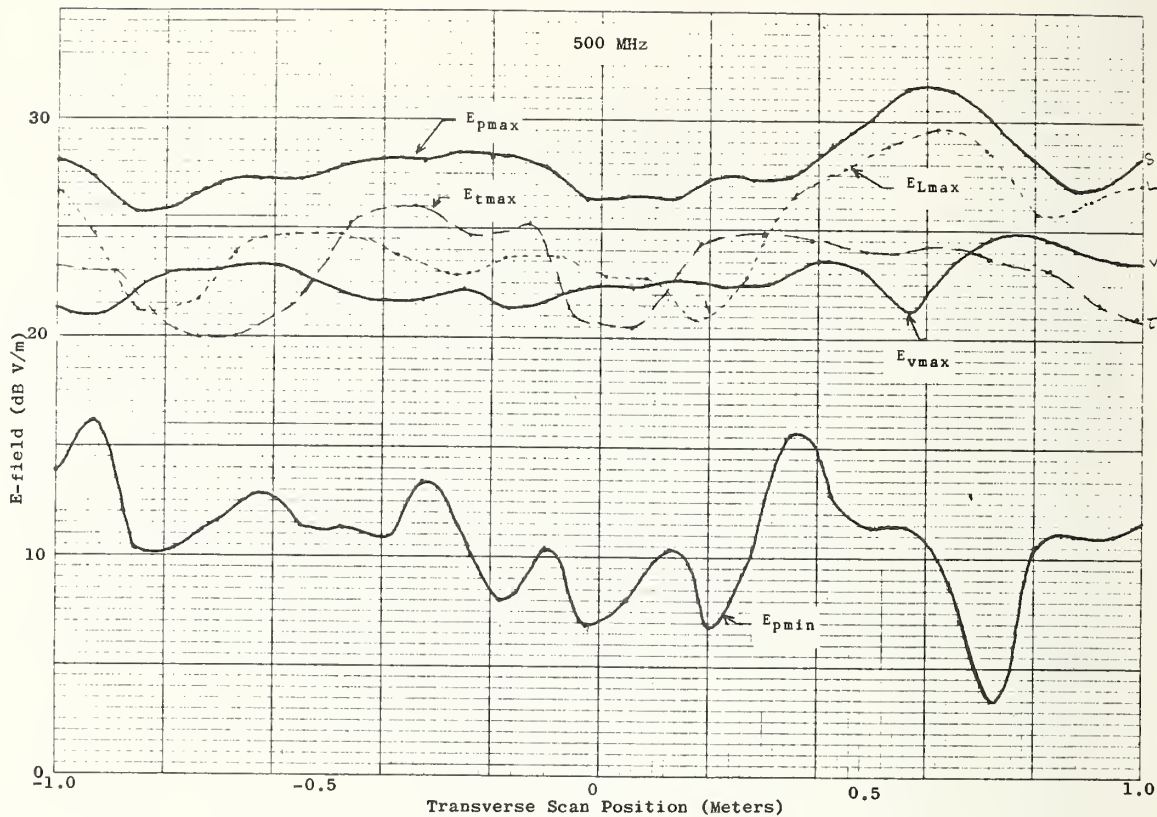


Figure 13c.

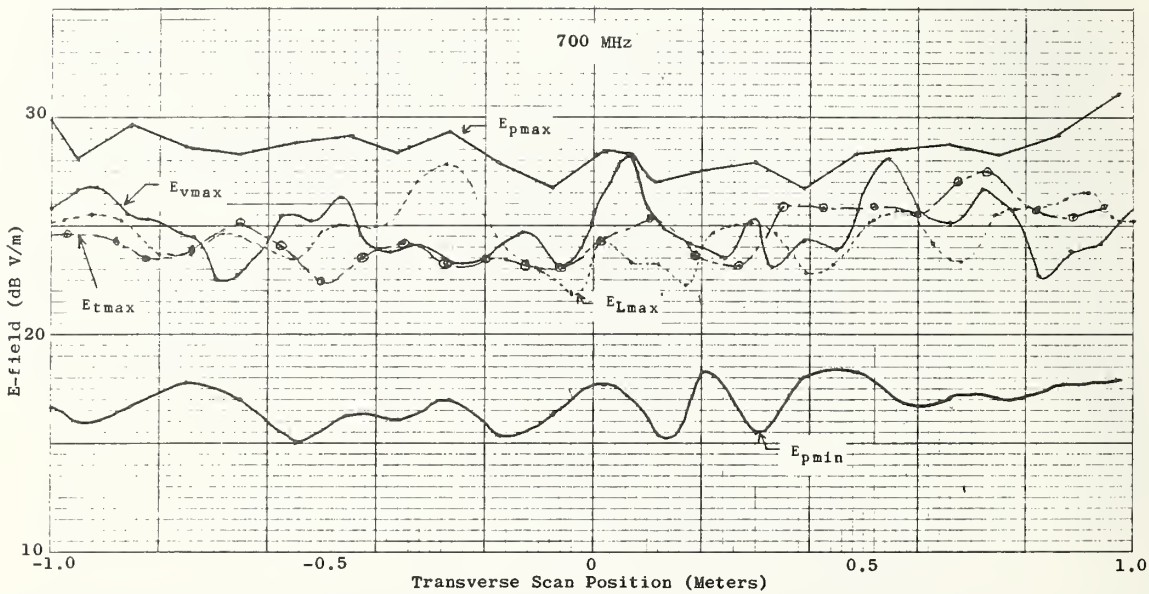


Figure 13d.

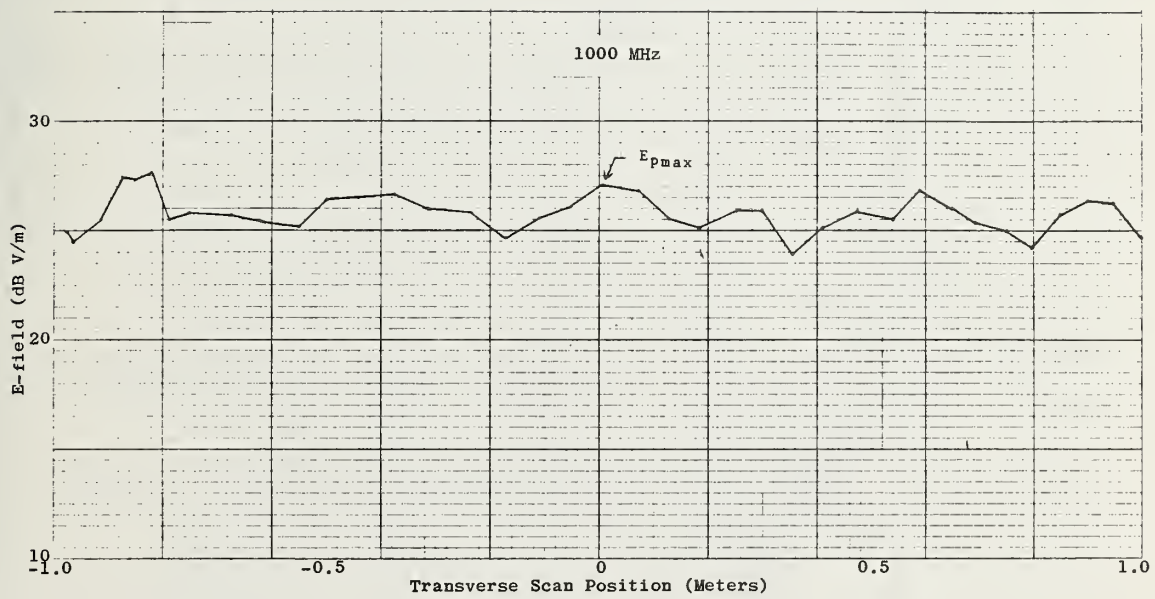


Figure 13e.

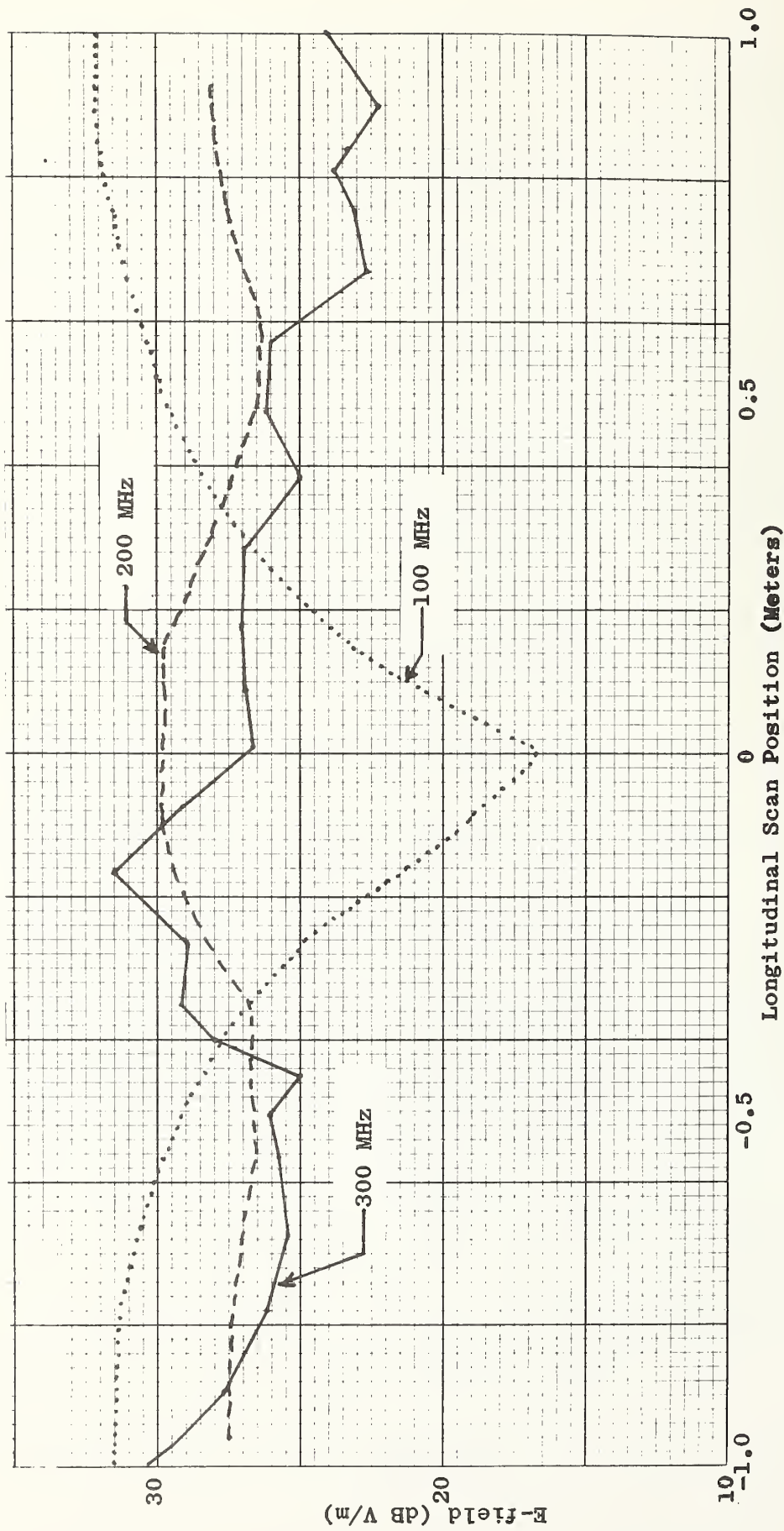


Figure 14. Results of E-field uniformity measurements taken along longitudinal scans through center of TEMEC test zone 0.914m above floor. Results are maximum amplitude of E-field obtained from measurement of hermitian magnitude of E-field using NBS probe.

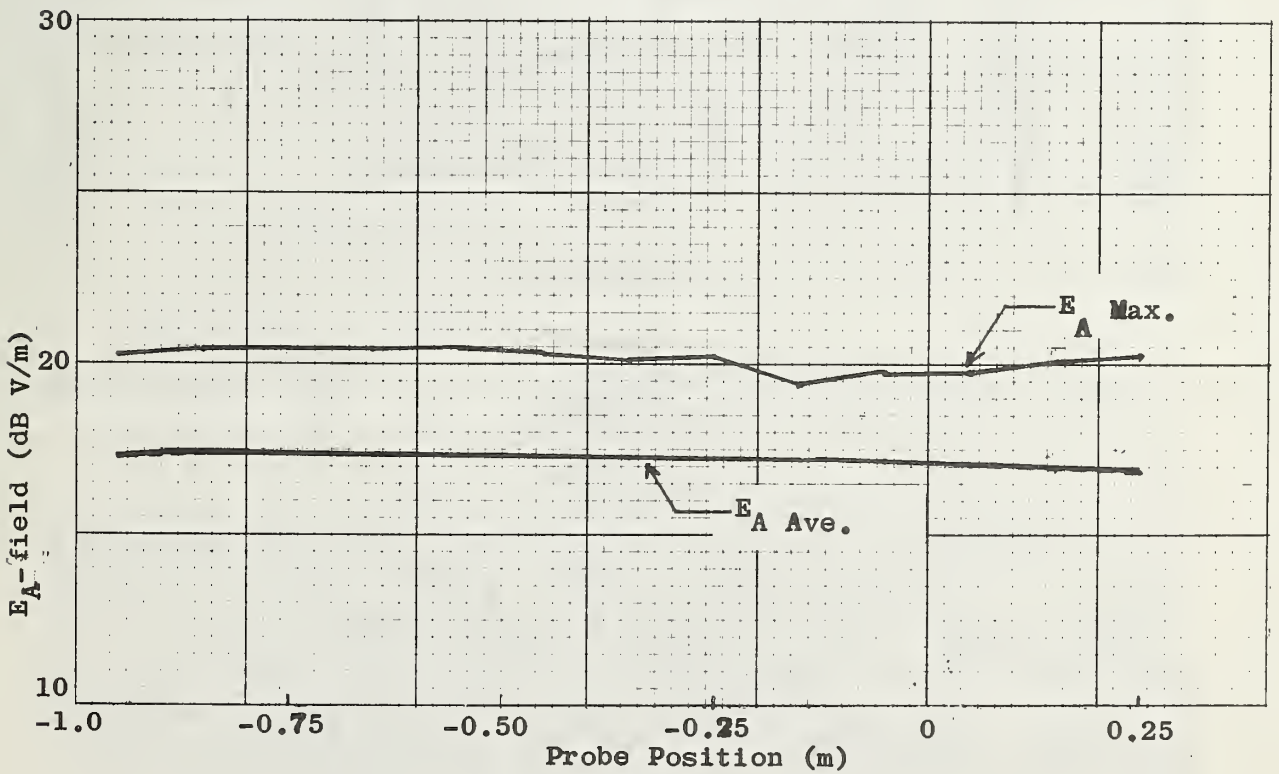
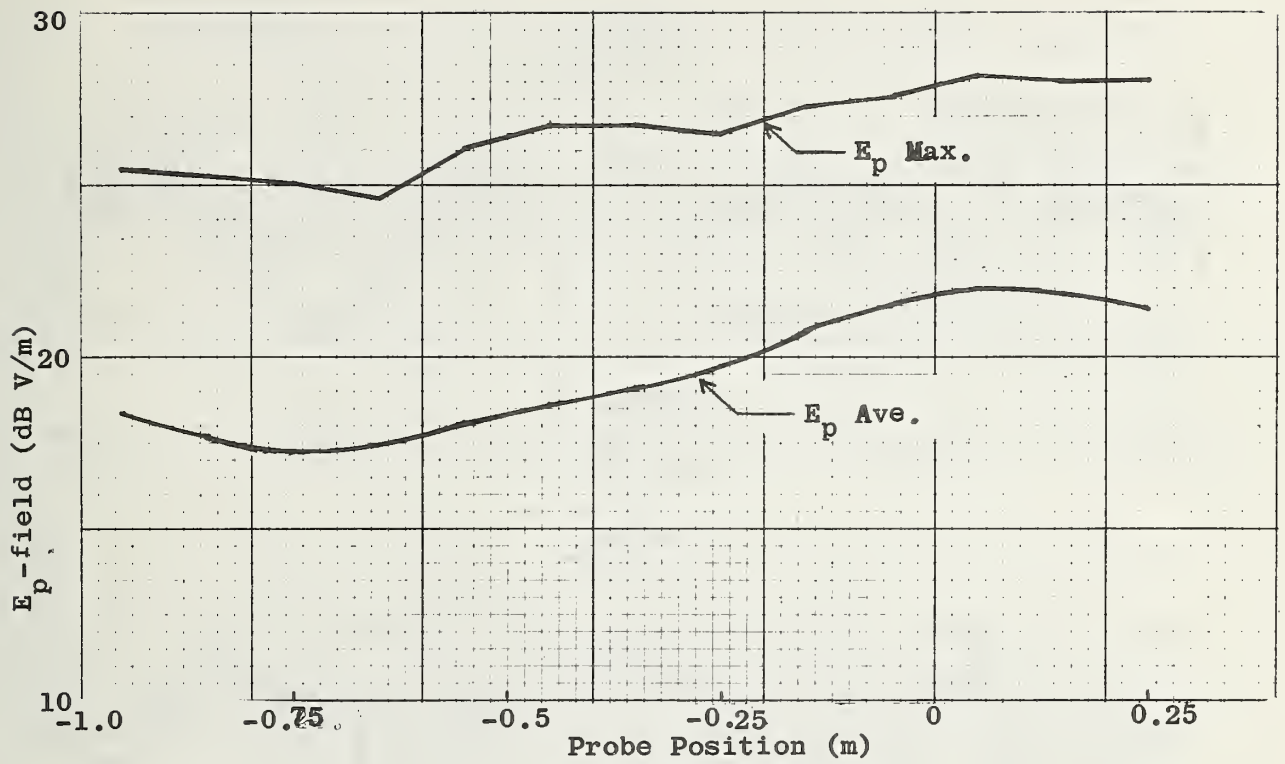
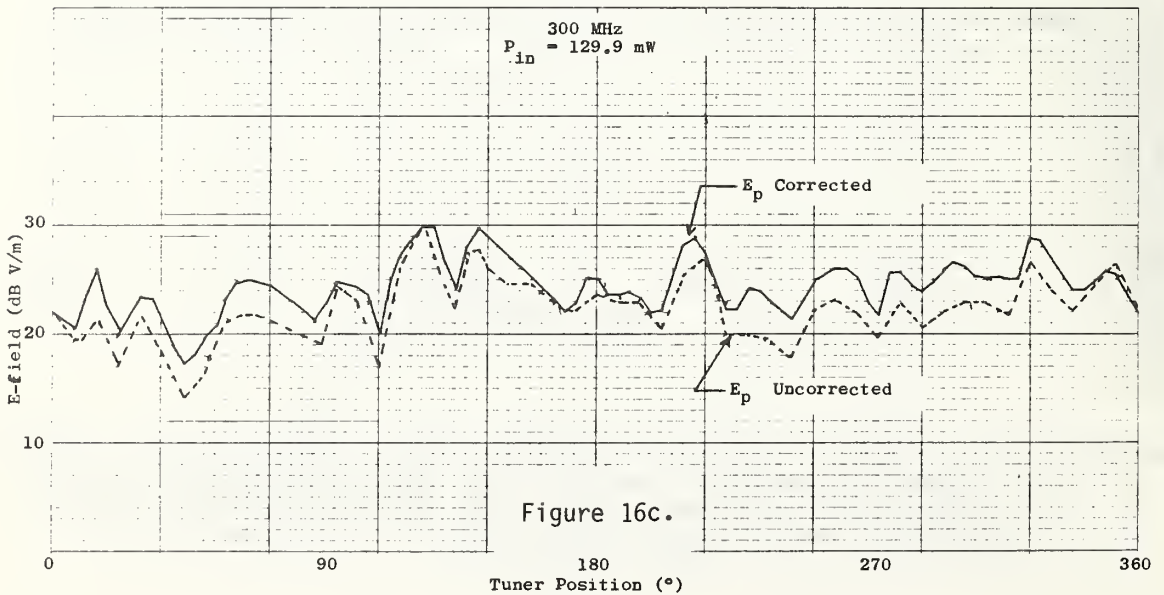
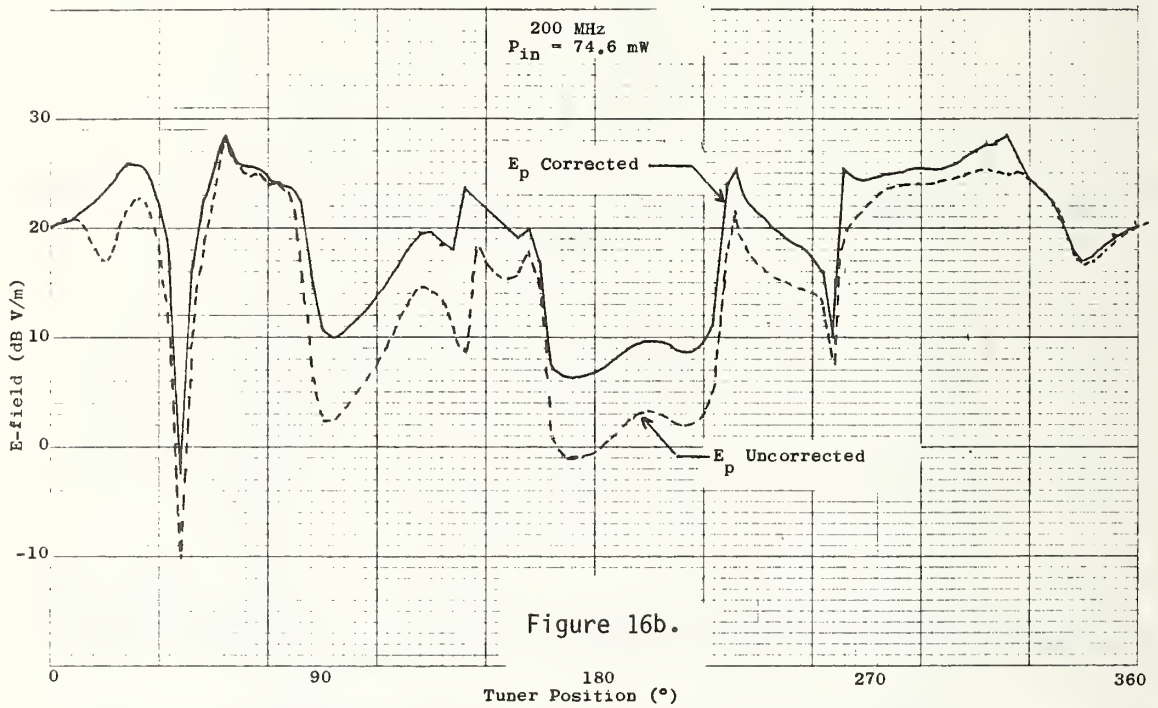
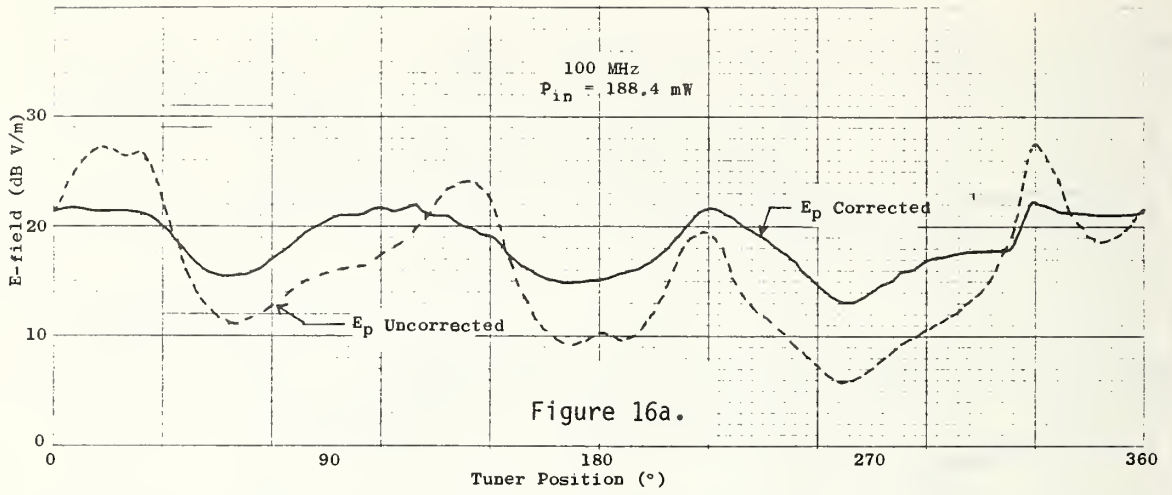


Figure 15. Results of E-field uniformity measurements made using NBS isotropic probe at 200 MHz. Computer based system used to correct for changes in net input power as a function of tuner and probe position. Scan made along length of chamber (longitudinal) through center of TEMEC test zone 0.914m above floor.



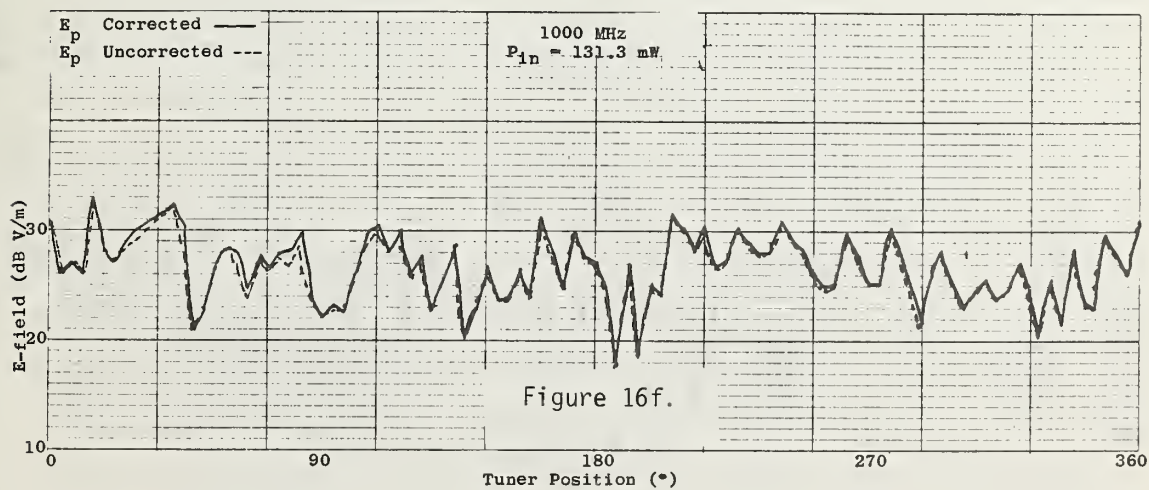
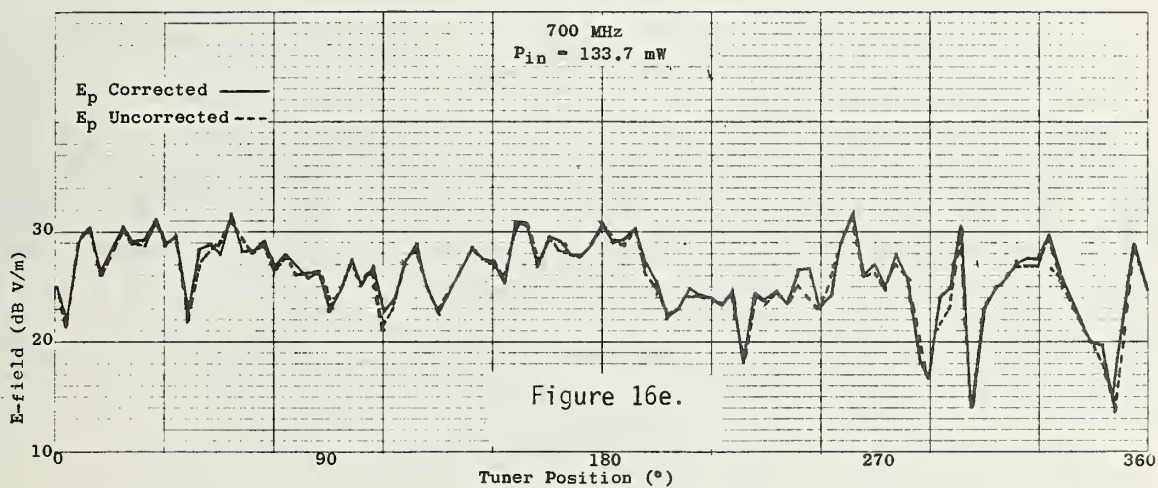
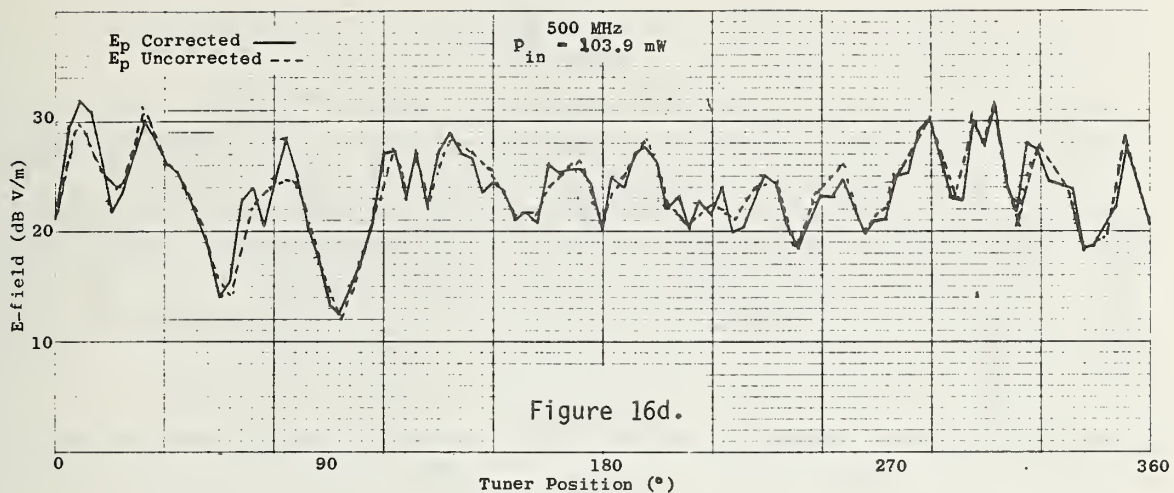
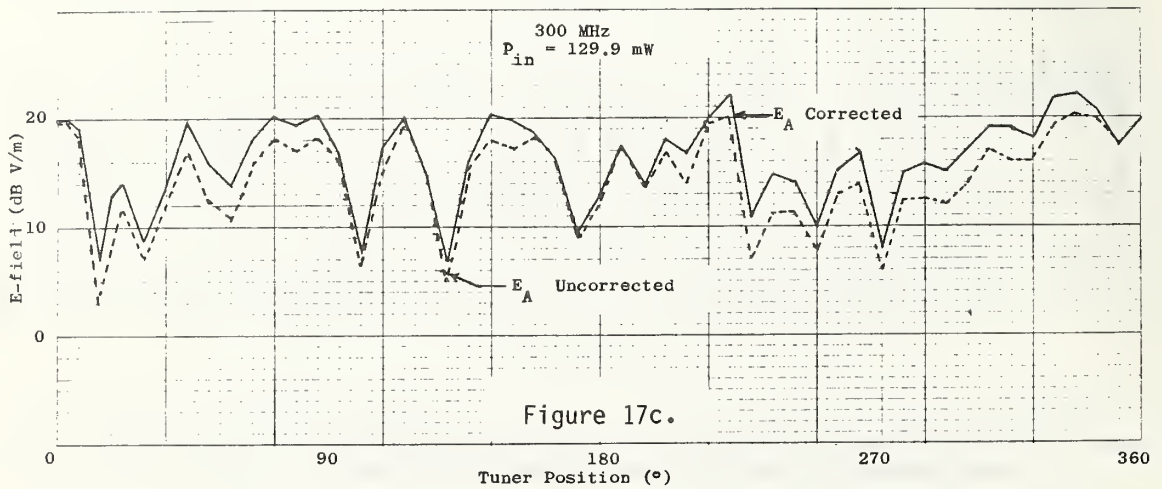
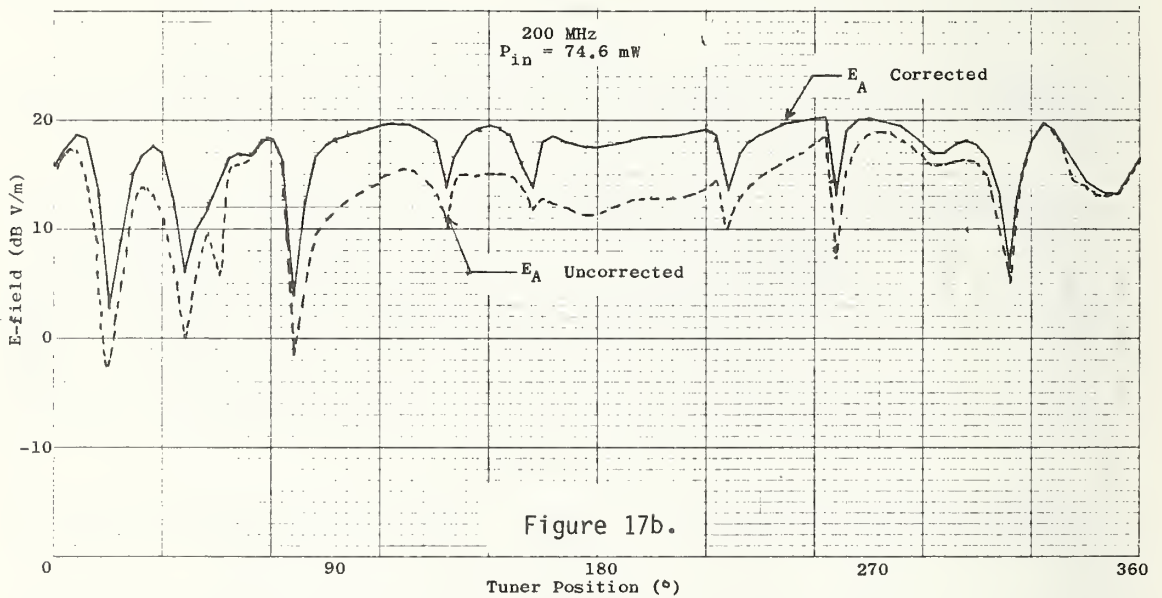
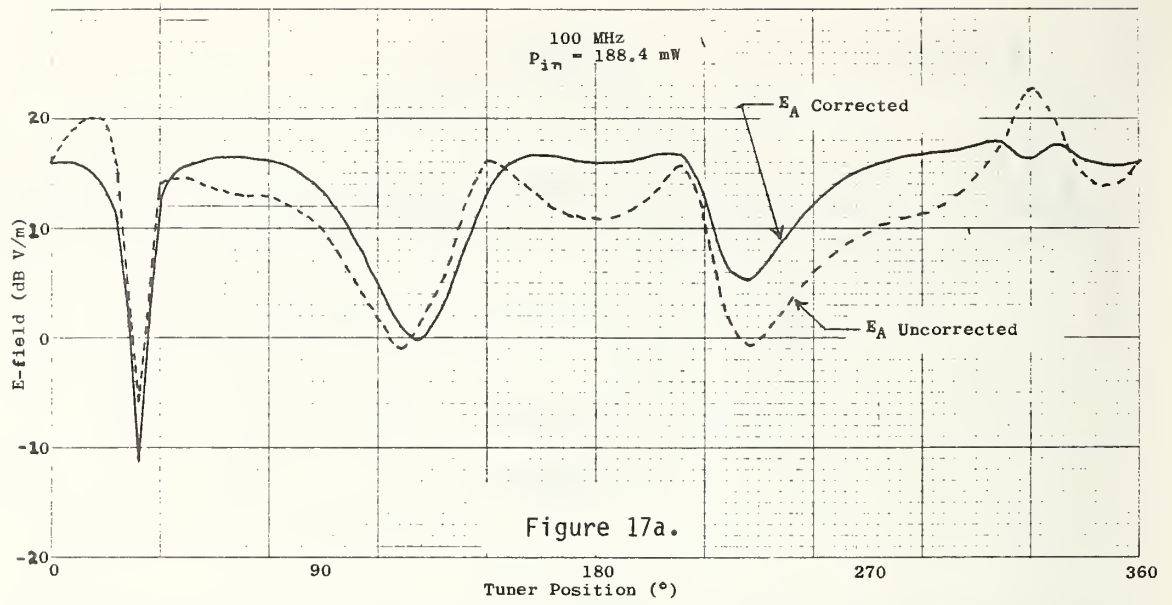


Figure 16. E-field amplitude inside TEMEC as determined from NBS calibrated isotropic probe measurements. Probe located at center of chamber.



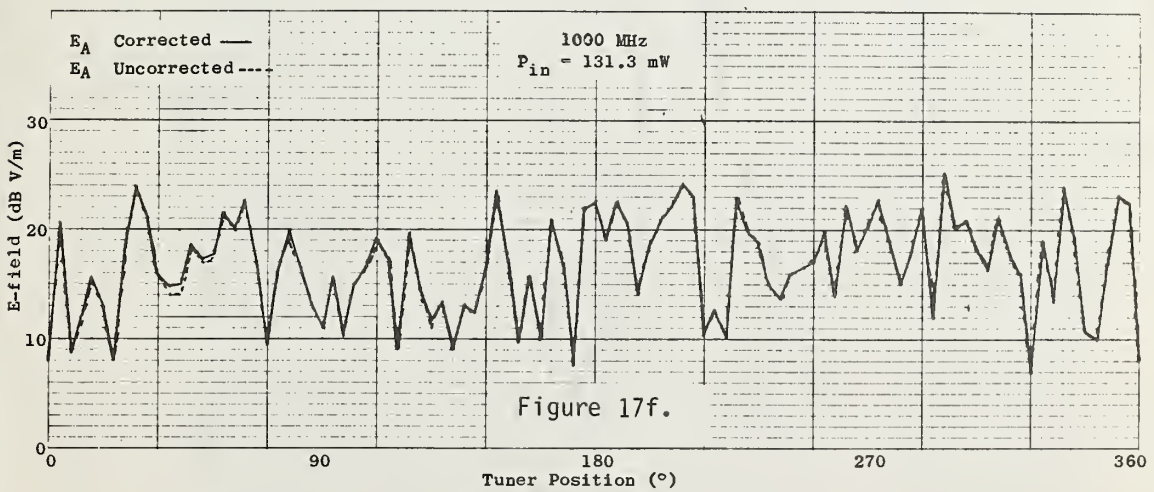
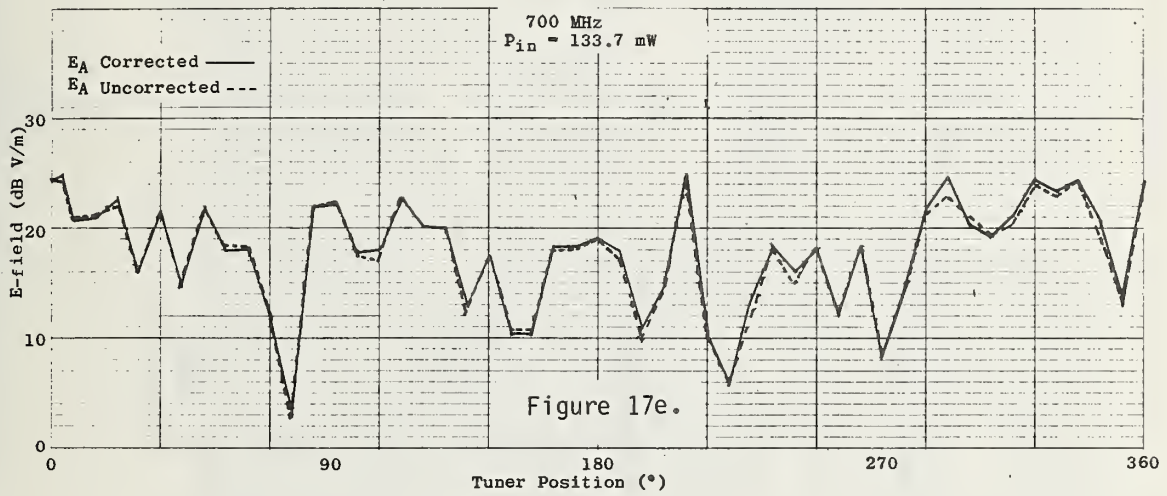
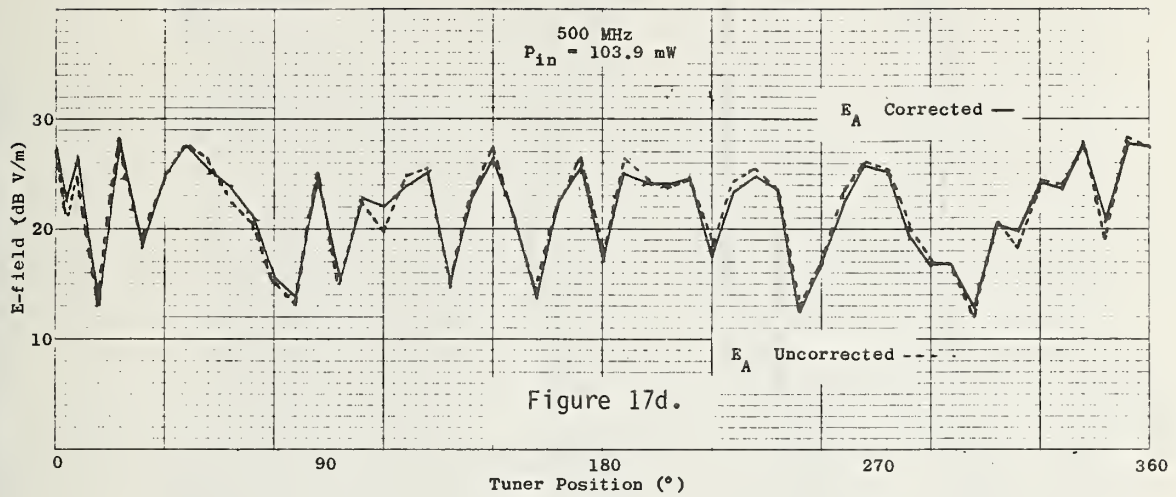


Figure 17. E-field amplitude inside TEMEC as determined from receiving antenna output power measurements.

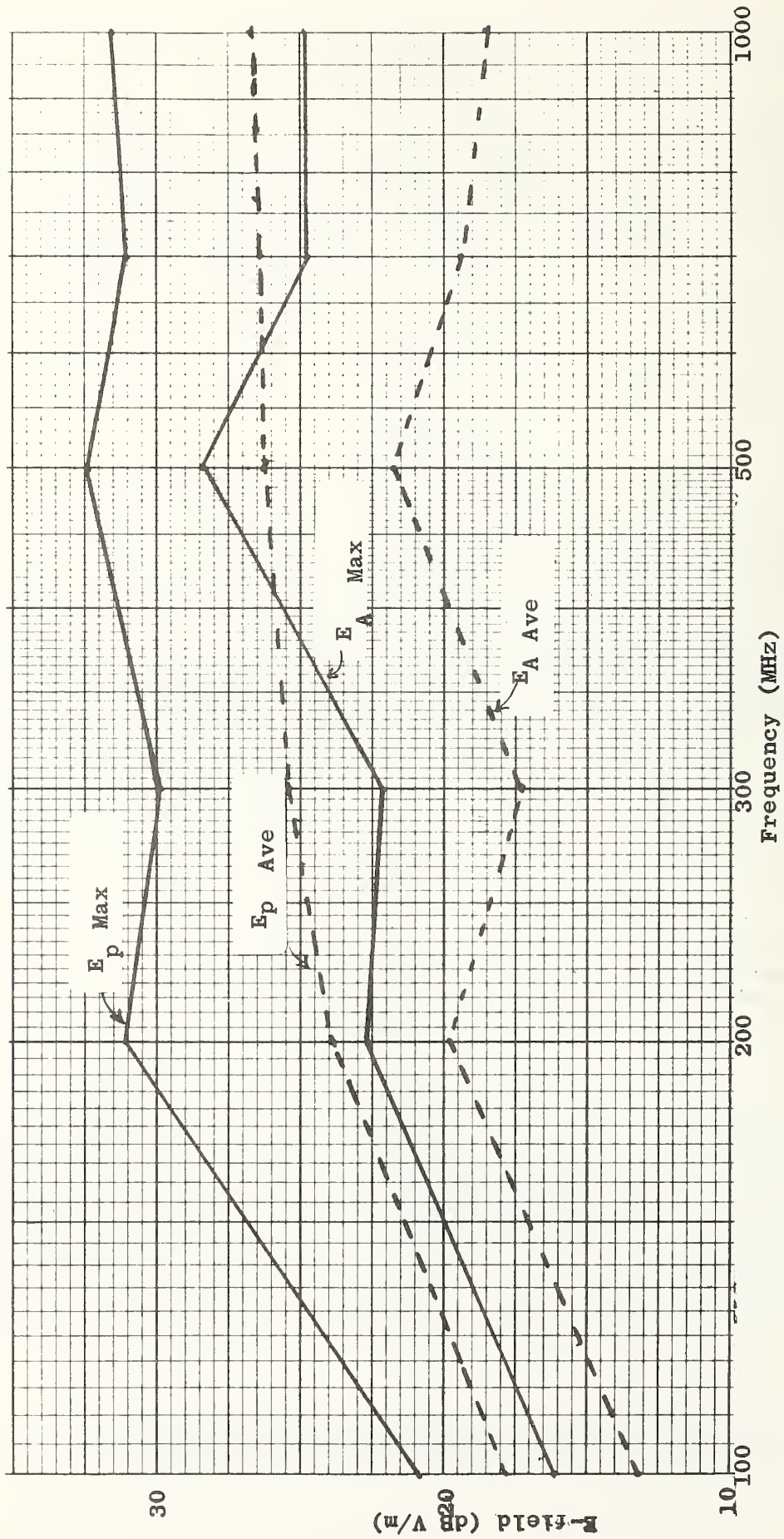


Figure 18. Maximum and average E-field in TEMEC chamber as determined by NBS calibrated probe and receiving antenna power measurements. E_p determined from NBS probe measurements. E_A determined from receiving antenna power measurements.

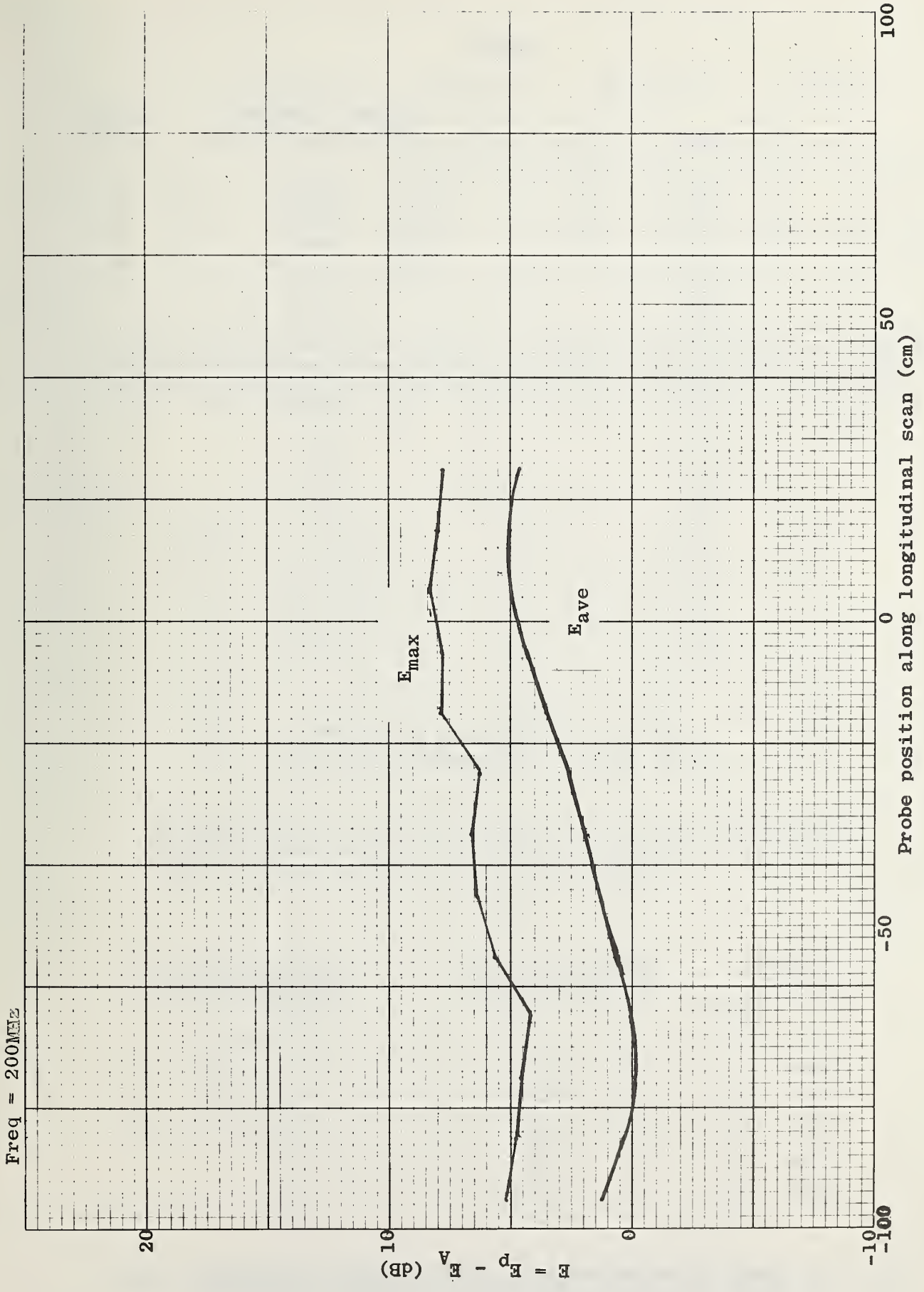


Figure 19. Difference between E-field inside TEMEC as determined by NBS probe and receiving antenna power as a function of probe position along a longitudinal scan at center of test zone one meter above floor. Probe motion is from door end (receiving antenna location) toward transmit antenna (back).

TABLE 1

<u>Mode</u>	<u>Resonant Frequency MHz</u>
f ₀₁₁	52.97
f ₀₁₂	63.00
f ₁₀₁	64.55
f ₁₀₂	73.00
f ₀₁₃	76.85
f ₁₁₀	78.73
f ₁₁₁	81.15
f ₁₀₃	85.25
f ₁₁₂	88.02
f ₁₁₃	98.41
f ₀₂₁	100.31
f ₀₂₂	105.95
f ₀₂₃	114.73
f ₁₂₀	116.00
f ₁₂₁	117.65
f ₂₀₁	124.52

Potential resonant modes inside TEMEC
(2.44m x 3.05m x 7.62m chamber) below 125 MHz

TABLE 2

<u>Frequency MHz</u>	<u>Transverse Scan E- Field Variation dB</u>	<u>Longitudinal Scan E- Field Variation dB</u>
100		15.3
200	6.5	3.5
300	5.7	9.3
500	5.9	
700	4.3	
1000	3.7	

Summary of maximum variation in E-field along scans through
TEMEC test zone. Scans ± 1 meter from center of chamber.
E-field measured using NBS isotropic probe.

TABLE 3

Frequency MHz	$S_d = E_V^2 + E_L^2 + E_t^2$ (dB V/m)			E_V (dB V/m)			E_L (dB V/m)			E_t (dB V/m)		
	Max.	Min.	Δ	Max.	Min.	Δ	Max.	Min.	Δ	Max.	Min.	Δ
200	30.1	23.6	6.5	26.9	20.1	6.8	25.5	17.8	7.7	27.5	15.8	11.7
300	29.5	23.9	5.6	27.9	20.3	7.6	23.2	18.0	5.2	26.5	17.0	9.5
500	31.6	25.7	5.9	24.9	21.0	3.9	29.6	20.9	8.7	26.0	20.0	6.0
700	31.1	26.7	4.4	28.3	22.5	5.8	27.8	21.9	5.9	27.5	22.4	5.1

Comparison of maximum E-field determined from NBS probe measurements made with a single dipole switched on and with all 3 orthogonal dipoles switched on (isotropic). Data gives maximum and minimum values of maximum E-field determined for a complete rotation of the mode tuner at discrete points along a transverse scan across the width of TEMEC (i.e., data shows influence of polarization of field in chamber).

TABLE 4

Frequency MHz	E_p Max dB	E_p Ave dB	E_A Max dB	E_A Ave dB
100	4.8	0.1	4.7	1.0
200	0.1	3.2	0.8	2.7
300	0.2	1.6	1.7	1.6
500	0.4	0	2.2	0.25
700	0.2	0.8	0.7	0.3
1000	0	0.15	0.35	0.2

Difference between E-field determined from probe and receiving antenna measurements with and without correcting for net input power changes to transmitting antenna (i.e., error possible from failure to normalize probe and antenna output to net input power changes).

TABLE 5

Frequency MHz	ΔE_{max} dB	ΔE_{ave} dB
100	4.3	4.5
200	8.0	4.5
300	7.6	7.5
500	3.9	4.0
700	6.8	7.0
1000	7.5	8.2

Summary of difference between E-field amplitude determination inside TEMEC using NBS calibrated probe, E_p and receiving antenna, E_A . $\Delta E = E_p - E_A$

U.S. DEPT. OF COMM. BIBLIOGRAPHIC DATA SHEET <i>(See instructions)</i>	1. PUBLICATION OR REPORT NO. NBSIR 81-1638	2. Performing Organ. Report No.	3. Publication Date February 1981
4. TITLE AND SUBTITLE <p style="text-align: center;">Evaluation of A Reverberation Chamber Facility for Performing EM Radiated Fields Susceptibility Measurements</p>			
5. AUTHOR(S) Myron L. Crawford			
6. PERFORMING ORGANIZATION <i>(If joint or other than NBS, see instructions)</i> NATIONAL BUREAU OF STANDARDS DEPARTMENT OF COMMERCE WASHINGTON, D.C. 20234			7. Contract/Grant No. 8. Type of Report & Period Covered
9. SPONSORING ORGANIZATION NAME AND COMPLETE ADDRESS <i>(Street, City, State, ZIP)</i> U. S. Navy Pacific Missile Test Center Pt. Mugu, California 93041			
10. SUPPLEMENTARY NOTES <input type="checkbox"/> Document describes a computer program; SF-185, FIPS Software Summary, is attached.			
11. ABSTRACT <i>(A 200-word or less factual summary of most significant information. If document includes a significant bibliography or literature survey, mention it here)</i> <p>This report describes measurement procedures and results for evaluation of a large 2.44m x 3.05m x 7.62m reverberating chamber facility in the frequency range (100-1000) MHz. This facility, referred to as a translational electromagnetic environment chamber, "TEMEC", is a mode tuned chamber developed for use in measuring electronic equipment susceptibility to EM radiated fields. A brief description of mode tuned cavity theory is given along with a description of the TEMEC measurement setup and the National Bureau of Standards modification of this setup for analysis and evaluation purposes. Measurements described include: (1) evaluation of the chamber's transmitting and receiving antenna voltage standing wave ratio; (2) measurement of the chamber's insertion loss or coupling efficiency versus frequency; (3) determination of E-field uniformity in the chamber test zone versus frequency; and (4) determination of the absolute amplitude calibration accuracy of the test fields in the chamber based upon the receiving antenna received power measurements.</p> <p>Conclusions given indicate the chamber may be useful for performing electro-magnetic susceptibility measurements at frequencies down to 200 MHz. E-field variations (time averaged) in the chamber's test zone decrease from approximately 10 dB at 200-300 MHz to less than 3.7 dB at 1000 MHz and are anticipated to be less than 2 dB above 2 GHz. The uncertainty in establishing the absolute E-field amplitude in the chamber test zone is estimated to be less than 10 dB.</p>			
12. KEY WORDS <i>(Six to twelve entries; alphabetical order; capitalize only proper names; and separate key words by semicolons)</i> Electromagnetic radiated susceptibility measurements; mode tuned chamber; resonant cavity.			
13. AVAILABILITY <input checked="" type="checkbox"/> Unlimited <input type="checkbox"/> For Official Distribution. Do Not Release to NTIS <input type="checkbox"/> Order From Superintendent of Documents, U.S. Government Printing Office, Washington, D.C. 20402. <input checked="" type="checkbox"/> Order From National Technical Information Service (NTIS), Springfield, VA. 22161			14. NO. OF PRINTED PAGES <p style="text-align: center;">44</p> 15. Price <p style="text-align: center;">\$6.50</p>

